# Acoustics

Lonny L. Thompson[1] and Peter M. Pinsky[2]

[1] *Department of Mechanical Engineering, Clemson University*
*Clemson, South Carolina, 29634-0921, USA*
[2] *Mechanical Engineering Department, Stanford University*
*Durand 261, Stanford, CA 94305-4040, USA*

ABSTRACT

State-of-the-art computational methods for linear acoustics are reviewed. The equations of linear acoustics are summarized and then transformed to the frequency domain for time-harmonic waves governed by the Helmholtz equation. Two major current challenges in the field are specifically addressed: Numerical dispersion errors that arise in the approximation of short unresolved waves, polluting resolved scales, and requiring a large computational effort; and the effective treatment of unbounded domains by domain-based methods. A discussion of the indefinite sesquilinear forms in the corresponding weak form are summarized. *A priori* error estimates, including both dispersion (phase error) and global pollution effects for moderate to large wave numbers in finite element methods are discussed. Stabilized and other wave-based discretization methods are reviewed. Domain based methods for modeling exterior domains are described including Dirichlet-to-Neumann (DtN) methods, absorbing boundary conditions, infinite elements, and the perfectly matched layer (PML). Efficient equation solving methods for the resulting complex-symmetric, (non-Hermitian) matrix systems are discussed including parallel iterative methods and domain decomposition methods including the FETI-H method. Numerical methods for direct solution of the acoustic wave equation in the time-domain are reviewed.

KEY WORDS: acoustics; wave equation; Helmholtz equation; finite element methods; Dirichlet-to-Neumann (DtN) boundary conditions, nonreflecting boundary conditions; absorbing boundary conditions; perfectly matched layer; infinite elements; domain decomposition methods.

Contents



*Encyclopedia of Computational Mechanics*. Edited by Erwin Stein, René de Borst and Thomas J.R. Hughes.

## 1. INTRODUCTION

Computational methods for acoustics has been an active research area for almost half a century with many advances occurring in the last decade. The topic of acoustics is wide ranging and includes both radiation and scattering of sound waves in fluids such as air and water and their interaction with vibrating structures. Due to difficulties in accurately resolving oscillating wave solutions at higher frequencies, many alternative and creative numerical methods have been proposed including stabilized finite element methods, and other wave-based discretization methods. The exterior acoustics problem in unbounded domains is an important application area which presents a special challenge for numerical methods. The dominating numerical methods for acoustic waves in unbounded domains can be divided into four main categories: boundary integral (element) methods, infinite elements, absorbing layers, and absorbing or nonreflecting boundary conditions. The method of choice depends on the shape and complexity of the scattering object, inhomogeneities, frequency range, and resolution requirements, among other parameters. Many of the methods developed for computational acoustics have been generalized to other applications with wave solutions, including electromagnetics, elastodynamics, geophysics, etc.

In this Chapter, state-of-the-art computational methods for linear acoustics are reviewed. Two major current difficulties in the field are specifically addressed: Numerical dispersion

*Encyclopedia of Computational Mechanics*. Edited by Erwin Stein, René de Borst and Thomas J.R. Hughes.

errors that arise in the approximation of short unresolved waves, polluting resolved scales, and requiring a large computational effort; and the effective treatment of unbounded domains. Emphasis is placed on methods for solving the Helmholtz equation governing time-harmonic acoustic waves in unbounded domains since this is often the most challenging, offering many creative alternatives for solution. Domain based finite element methods for modeling exterior domains are described including Dirichlet-to-Neumann (DtN) methods, absorbing boundary conditions, infinite elements, and the perfectly matched layer (PML). The indefinite sesquilinear forms arising from the weak form of the variational problem for the Helmholtz equation is described and discussed. Topics include discussion of *a priori* error estimates; both dispersion (phase error) and global pollution effects for moderate to large wave numbers in the h-version, hp-version, and spectral-version of the FEM as well as stabilized methods for the numerical solution of the Helmholtz equation governing time-harmonic acoustic waves. Efficient equation solving methods for the resulting complex-symmetric, (non-Hermitian) matrix systems are discussed including parallel iterative methods and domain decomposition methods such as the FETI-H method. A review of numerical methods for direct solution of the acoustic wave equation in the time-domain is also given.

Starting from the Euler equations and constitutive behavior for small motions of a compressible, adiabatic, and inviscid fluid the system of first-order hyperbolic equations for linear variations of acoustic pressure and velocity is reviewed in Section 2. Eliminating velocity variables leads to the scalar wave equation governing the acoustic pressure or a velocity potential. In Section 3 the equations of linear acoustics are then transformed to the frequency domain for time-harmonic waves governed by the Helmholtz equation. Discretization methods for the corresponding indefinite sesquilinear variational forms are discussed in Section 4. A dispersion analysis of the Galerkin finite element method for piecewise linear interpolation in a one-dimensional setting is given to illustrate the numerical phase error in the approximate solution. For both low-order and high-order polynomial finite element basis functions, rules of thumb arising from mathematical and numerical analysis are summarized for controlling dispersion error and global pollution errors at moderate to high wavenumbers. Galerkin-least-squares (GLS) and other wave-based discretization methods designed to reduce dispersion and pollution error are reviewed. In Section 5, the exterior problem in unbounded domains is described. A detailed derivation of the exact DtN non-reflecting boundary condition is given in Section 6. In Section 7 improved modified DtN operators on spherical nonreflecting boundaries, suitable for finite element discretization are derived in order to form a foundation for understanding uniqueness requirements and generalizations to other geometries. Efficient finite element implementation including sparse iterative solution methods are addressed. In Section 8, infinite elements for acoustic waves are described; both conjugated and unconjugated test functions are considered. In Section 9 perfectly-matched-layer (PML) methods for the Helmholtz equation in a weak form suitable for finite element discretization are described. Methods for accelerating multi-frequency solutions are given in Section 10. Parallel iterative solution methods for both sparse and DtN matrices on distributed-memory systems are addressed in Section 11. In Section 12 the FETI-H domain decomposition method based on Lagrange multipliers and regularization matrices for the Helmholtz equation is described. Finally, numerical methods for direct solution of the time-dependent acoustic equations are reviewed in Section 13.

The chapter provides an overview of many of the most important recent developments in computational acoustics, but due to page constraints, is not intended to be a complete

*Encyclopedia of Computational Mechanics*. Edited by Erwin Stein, René de Borst and Thomas J.R. Hughes.

accounting of all references and methods in the field. Methods for acoustic waves in three-dimensions have been emphasized in the presentation. Two-dimensional waves display a fundamentally different solution behavior; numerical methods for two-dimensional acoustics problems can be found in (Givoli, 1992; Givoli, 1999; Harari *et al.*, 1996) and other works from many of the authors listed in the references. Other important topics in computational acoustics not discussed include finite and boundary element solution for acoustic waveguides (Givoli, 1999; Filippi *et al.*, 1999; Ciskowski and Brebbia, 1991; von Estorff, 2000), structural acoustics (Harari *et al.*, 1996; Junger and Feit, 1993), adaptive methods for the Helmholtz equation (Stewart and Hughes, 1997; Bouillard and Ihlenburg, 1999), acoustic inverse problems (Farhat, Tezaur and Djellouli, 2002), and sensitivity analysis and optimization, (Feijoo *et al.*, 2001; Marburg, 2002).

## 2. ACOUSTIC FIELD EQUATIONS

For an ideal linear compressible fluid, assumed to be inviscid, the stress tensor takes the form

$$\boldsymbol{\tau} = -p\boldsymbol{I} = \lambda(\nabla \cdot \boldsymbol{u})\boldsymbol{I} \tag{1}$$

where $p$ is the acoustic pressure (the pressure in excess of any static pressure), $\boldsymbol{u}$ is the displacement vector, $\lambda$ is the elastic constant (bulk modulus), and $\boldsymbol{I}$ is the unit tensor. Define the velocity vector as the time derivative of displacement $\boldsymbol{v} = \dot{\boldsymbol{u}}$, and $\lambda = \rho c^2$, where $c$ is the wave speed and $\rho$ is the ambient density. It follows that the constitutive behavior is,

$$p = -\lambda \nabla \cdot \boldsymbol{u}, \quad \text{or} \quad \dot{p} = -\rho c^2 \nabla \cdot \boldsymbol{v} \tag{2}$$

This equation represents the linearized conservation of mass for the condition of constant entropy. The equilibrium equations for small motions of a compressible, adiabatic fluid may be expressed as,

$$\rho \dot{\boldsymbol{v}} - \nabla \cdot \boldsymbol{\tau} = \boldsymbol{f} \tag{3}$$

where $\boldsymbol{f}$ is a body force. Substituting (1) into (3) we arrive at the Euler equations for the acoustic fluid,

$$\rho \dot{\boldsymbol{v}} + \nabla p = \boldsymbol{f} \tag{4}$$

The two equations (2) and (4) give a complete set of linear equations for the velocity and pressure unknowns, $\boldsymbol{U} = (\boldsymbol{v}, p)$. Expressed in state vector form, the equations form a classical system of first-order hyperbolic equations,

$$\frac{\partial \boldsymbol{U}}{\partial t} + \sum_{i=1}^{3} \boldsymbol{A}_i \frac{\partial \boldsymbol{U}}{\partial x_i} = \boldsymbol{F} \tag{5}$$

where the $4 \times 4$ matrices $\boldsymbol{A}_i$ depend on the physical parameters $\rho$ and $c$, and $\boldsymbol{F} = (\boldsymbol{f}/\rho, 0)$.

Combining (2) and (4) and eliminating velocity we arrive at the generalized scalar wave equation for the acoustic pressure (Pierce, 1998):

$$\nabla \cdot \left( \frac{1}{\rho} \nabla p \right) - \frac{1}{\rho c^2} \ddot{p} = f, \qquad f = \nabla \cdot \left( \frac{1}{\rho} \boldsymbol{f} \right) \tag{6}$$

*Encyclopedia of Computational Mechanics*. Edited by Erwin Stein, René de Borst and Thomas J.R. Hughes.

For a fluid with constant ambient density $\rho$, (6) reduces to the classical wave equation,

$$\nabla^2 p - \frac{1}{c^2}\ddot{p} = f \tag{7}$$

where $f = \nabla \cdot \boldsymbol{f}$. The wave equation is often written in operator form as,

$$\Box^2 p = \left(\nabla^2 - \frac{1}{c^2}\frac{\partial^2}{\partial t^2}\right) p = f \tag{8}$$

For irrotational flow, neglecting body forces and assuming constant $\rho$, an alternate form may be used. Taking the curl of (4), it is clear that the equations admit solutions $\nabla \times \boldsymbol{v} = 0$, and can thus be defined in terms of a *velocity potential* such that $\boldsymbol{v} = \nabla\phi$. Equation (4) is then satisfied with

$$p = -\rho\dot{\phi}. \tag{9}$$

Substituting $\boldsymbol{v} = \nabla\phi$ into (2) and combining with (9) we arrive at the wave equation for the scalar velocity potential, $\Box^2\phi = 0$.

### *2.1. Boundary Conditions at Interfaces*

For the acoustic model, viscous forces are neglected, thus interface boundary conditions only require continuity of the normal component of velocity and traction (pressure). The continuity of traction may be expressed as,

$$\boldsymbol{\tau} \cdot \boldsymbol{n} = -p\boldsymbol{n} = \rho\dot{\phi}\boldsymbol{n} \tag{10}$$

The kinematic boundary condition representing the continuity of the normal component of velocity may be expressed as,

$$\nabla\phi \cdot \boldsymbol{n} = \boldsymbol{v} \cdot \boldsymbol{n} \tag{11}$$

Taking the time derivative, and making use of the equations of motion (4), continuity of the normal component of acceleration may be expressed in terms of the normal derivative of pressure as,

$$\nabla p \cdot \boldsymbol{n} = -\rho\dot{\boldsymbol{v}} \cdot \boldsymbol{n} \tag{12}$$

For a rigid nonmoving surface, the normal component of velocity and acceleration must vanish, but no restrictions are placed on tangential components.

## 3. TIME-HARMONIC WAVES AND THE HELMHOLTZ EQUATION

Plane waves of angular frequency $\omega$, with units of radians traveling in the direction $\boldsymbol{n}$ at the sound speed $c$, can be expressed as the sinusoidal wave function,

$$p = |p| \cos\left[(k\boldsymbol{x} \cdot \boldsymbol{n} - \omega t) + \varphi\right] \tag{13}$$

where $|p|$ is the amplitude, $\varphi$ is a phase constant, and $k = \omega/c$ is the *wavenumber*. The *wavelength* with units of length is defined by $\lambda = 2\pi/k$. The dual measure of period is defined by $T = 2\pi/\omega$ and has units of time.

It is convenient to express the acoustic variables in complex-number representation,

$$p = \mathrm{Re}\left\{\hat{p}(\boldsymbol{x})e^{-i\omega t}\right\}, \qquad i = \sqrt{-1} \tag{14}$$

*Encyclopedia of Computational Mechanics*. Edited by Erwin Stein, René de Borst and Thomas J.R. Hughes.

where $\hat{p}(\boldsymbol{x})$ is the complex amplitude. The notation 'real part', Re, is often suppressed for the sake of brevity; this convention will be used hereafter.

Using the complex exponential form, time-harmonic plane waves my be expressed as the sinusoidal wave train,

$$p = Ae^{i(k\boldsymbol{x}\cdot\boldsymbol{n}-\omega t)} = Ae^{i(\boldsymbol{k}\cdot\boldsymbol{x}-\omega t)} \tag{15}$$

Here, $A = |A|e^{i\varphi_A}$ is a complex number with magnitude $|A|$ and phase angle $\varphi_A$. The *wave vector* $\boldsymbol{k} = k\boldsymbol{n}$ is defined by the direction of the unit vector $\boldsymbol{n}$. The equation of constant phase $\xi(\boldsymbol{x}, t) = k\boldsymbol{x}\cdot\boldsymbol{n} - \omega t$ describes a moving surface. The wave vector $\boldsymbol{k} = k\boldsymbol{n} = \nabla\xi$ is orthogonal to the surface of constant phase, and represents the direction of wave propagation.

Assuming time-harmonic solutions, the linear wave equation (7) reduces to the Helmholtz equation in the frequency domain (Helmholtz, 1860):

$$\nabla^2\hat{p} + k^2\hat{p} = \hat{\boldsymbol{f}} \tag{16}$$

where $k = \omega/c$. Substituting (15) into (16) it is clear that the plane-wave solution satisfies the Helmholtz equation. The same reduced equation for the frequency dependent complex amplitude $\hat{p}(\boldsymbol{x};\omega)$, may be obtained from the Fourier transform; see e.g. (Williams, 1999),

$$\hat{p}(x;\omega) = \mathcal{F}[p(\boldsymbol{x}, t)] = \int_{-\infty}^{\infty} p(\boldsymbol{x}, t)e^{i\omega t}dt \tag{17}$$

The Fourier transform of the time derivative is, $\mathcal{F}[\frac{\partial p(t)}{\partial t}] = -i\omega\hat{p}(\omega)$, thus time derivatives are replaced using the substitution, $\frac{\partial}{\partial t} \to -i\omega$, $\frac{\partial^2}{\partial t^2} \to -\omega^2$.

For time-harmonic scattering and radiation, a general impedance condition on surface $S$ may be stated as,

$$\frac{\partial\hat{p}}{\partial n} + \beta\,(\hat{p} - g_1) = g_2, \qquad \boldsymbol{x} \text{ on } S \tag{18}$$

Here, $(\partial\hat{p}/\partial n) := \nabla\hat{p}\cdot\boldsymbol{n}$ is the exterior normal derivative, $\beta(\boldsymbol{x};k) \in \mathbb{C}$, and $g_1(\boldsymbol{x};k) \in \mathbb{C}$, $g_2(\boldsymbol{x};k) \in \mathbb{C}$ are given wavenumber-dependent complex valued functions. $\beta \to 0$ and $g_2 = 0$, represents a 'hard' or 'rigid' surface, where as $\beta \to \infty$ leads to the Dirichlet condition $\hat{p} = g_1$. In the case $g_1 = 0$, the Dirichlet condition represents a 'release' or 'soft' boundary.

In summary, for the Helmholtz equation (16) defined on a bounded domain $\Omega$ with general impedance condition (18) on surface $S$, the strong form of the boundary value problem for a given wavenumber $k$ is (S): Given the wavenumber-dependent source function $f(\boldsymbol{x};k)$, and boundary data $g_1(\boldsymbol{x};k)$, and $g_2(\boldsymbol{x};k)$, with constant $\beta(\boldsymbol{x};k)$, such that $0 \le |\beta| < \infty$; Find the complex-valued scalar field $u(\boldsymbol{x}) \in \mathbb{C}$, such that,

$$(\nabla^2 + k^2)\,u = f, \qquad \text{in } \Omega \tag{19}$$

$$u = g_1, \qquad \text{on } S_1 \tag{20}$$

$$\frac{\partial u}{\partial n} + \beta\,u = g_2, \qquad \text{on } S_2 \tag{21}$$

Here, $u(\boldsymbol{x})$ represents the spatial part of the acoustic pressure or velocity potential, and $S = \overline{S_1 \cup S_2}$, $S_1 \cap S_2 = 0$.

*Encyclopedia of Computational Mechanics*. Edited by Erwin Stein, René de Borst and Thomas J.R. Hughes.

## 4. DISCRETIZATION METHODS FOR THE HELMHOLTZ EQUATION

Define the trial space of functions, $V = \{u \in H^1(\Omega),\ u = g_1 \text{ on } S_1\}$, and test (variation) space $V_0 = \{u \in H^1(\Omega),\ u = 0 \text{ on } S_1\}$. The weak form corresponding to equations (19), (21), and (20) is (W): find $u \in V$, such that, for all $w \in V_0$:

$$B(w\,,\,u) = F(w) \tag{22}$$

with sesquilinear form,

$$B(w\,,\,u) := \int_\Omega (\nabla \bar{w} \cdot \nabla u \,-\, k^2\,\bar{w}\,u)\,\mathrm{d}\boldsymbol{x} + \int_{S_2} \beta \bar{w}\,u\,\mathrm{d}\boldsymbol{s}, \tag{23}$$

and

$$F(w) := (w, g_2)_{L^2(S_2)} - (w, f)_{L^2(\Omega)} = \int_{S_2} \bar{w}\,g_2\,\mathrm{d}\boldsymbol{s} - \int_\Omega \bar{w}\,f\,\mathrm{d}\boldsymbol{x}$$

In the above, the bar indicates complex conjugate. For the purely Neumann boundary condition with $S = S_2$, then both test and trial spaces are equal to $H^1(\Omega)$.

Let $V^h \subset V$ and $V_0^h \subset V_0$ be finite dimensional linear spaces formed by a discretization, then the Galerkin form is: Find $u^h \in V^h$ such that $\forall\, w^h \in V_0^h$, $B(w^h, u^h) = F(w^h)$. Assuming a Galerkin approximation $u^h = v^h + g_1^h \in V^h$, such that $v^h \in V_0^h$, and

$$v^h(\boldsymbol{x}) = \sum_{i=1}^{N_{dof}} N_i(\boldsymbol{x})\,d_i,$$

where $N_i(\boldsymbol{x})$ are linearly independent basis (shape) functions with $N_{dof}$ unknown complex coefficients $d_i$, and similarly defining the test functions $w^h \in V_0^h$ as the linear span of basis functions $N_i \in V_0$ for $i = 1, \ldots, N_{dof}$, results in the complex-symmetric (non-Hermitian) matrix equation system,

$$[\boldsymbol{S} + \boldsymbol{S}_\beta - k^2\boldsymbol{M}]\,\boldsymbol{d} = \boldsymbol{f} \tag{24}$$

with matrices,

$$(\boldsymbol{S})_{ij} = \int_\Omega \nabla N_i \cdot \nabla N_j\,\mathrm{d}\boldsymbol{x}, \quad (\boldsymbol{S}_\beta)_{ij} = \int_{S_2} \beta N_i N_j\,\mathrm{d}\boldsymbol{s}, \quad (\boldsymbol{M})_{ij} = \int_\Omega N_i N_j\,\mathrm{d}\boldsymbol{x}, \tag{25}$$

and forcing vector, $(\boldsymbol{f})_i = (N_i, g_2)_{L^2(S_2)} - (N_i, f)_{L^2(\Omega)} - B(N_i, g_1^h)$. Often a large number of frequency (wavenumber) evaluations are required over a broad band to characterize the system response or when an inverse Fourier transform is needed to construct a corresponding time-domain solution. Since the 'dynamic stiffness matrix' $[\boldsymbol{S} + \boldsymbol{S}_\beta - k^2\boldsymbol{M}]$ is wavenumber-dependent, the solution generally involves a separate inversion at each wavenumber. For larger wavenumbers $k$, Galerkin solutions for the indefinite but coercive forms associated with the Helmholtz equation may behave erratically for small numbers of degrees-of-freedom $N_{dof}$ and start to display a convergence rate only after $N_{dof}$ has reached a critical number (Ihlenburg, 1998). For bounded domains, damped interior resonances corresponding to the eigenvalues of the Helmholtz operator are present. Fixing a particular measuring point, $u^h(\boldsymbol{x}_0; k) = v^h(\boldsymbol{x}_0; k) + g_1^h(\boldsymbol{x}_0; k)$, for a range of wavenumber $k$, the response function $H(k)$, relating the response of the system at one point $\boldsymbol{x}_0$ to the excitation $\boldsymbol{f}(k)$ is formed.

*Encyclopedia of Computational Mechanics*. Edited by Erwin Stein, René de Borst and Thomas J.R. Hughes.

*4.1. Galerkin Finite Element Methods*

Finite element methods partition the computational domain $\Omega$ into nonoverlapping subdomains (elements) $\Omega_e$ with continuous piece-wise polynomials. In the standard $h$-version, basis functions $N_i(\boldsymbol{x})$, associated with element nodes are $C^0$ continuous interpolation functions with compact support such that the unknown amplitudes take on the point values $d_i = u^h(\boldsymbol{x}_i)$. Accuracy of finite element approximations based on Galerkin's method are characterized by dispersion errors. In order to control dispersion (phase) error, the element size must be adapted to the wavenumber (frequency), i.e., the number of elements per wavelength measured by $kh = 2\pi h/\lambda$ must be held below a limit value. Here $h$ is a measure of the element size, for example, in two-dimensions $h = \sqrt{A_e}$, where $A_e$ is the element area might be used. In order to quantify the limiting value on the mesh resolution, a dispersion analysis can be performed.

For a uniform mesh of elements with piecewise linear interpolation in one-dimension, and neglecting boundary conditions, the system matrix $\boldsymbol{K}_\Omega = [\boldsymbol{S} - k^2\boldsymbol{M}]$, is tridiagonal; each interior equation corresponds to a repeated finite difference stencil centered at a typical node $j$. Neglecting source terms, the stencil can be written as,

$$B(\alpha)u_{j-1} + A(\alpha)u_j + B(\alpha)u_{j+1} = 0 \tag{26}$$

Assuming all elements to be of equal length $h$, the coefficients in (26) are,

$$A(\alpha) = 1 - \alpha^2/3, \qquad B(\alpha) = -1 + \alpha^2/6$$

In the above, $u_j = u^h(x_j)$, is the nodal solution, and $\alpha = kh$ is the non-dimensional wavenumber. The solution of the difference stencil (26) admits a propagating plane-wave solution of the form,

$$u^h(x_j) = u_0 e^{i\tilde{k}x_j}$$

where $\tilde{k}$ is the unknown numerical wave number, and (26) transforms into the algebraic equation,

$$B(\alpha)\lambda^{j-1} + 2A(\alpha)\lambda^j + B(\alpha)\lambda^{j+1} = 0$$

where $\lambda = e^{i\beta}$, $\beta = \tilde{k}h$. Simplifying results in the dispersion relation relating the numerical wavenumber to the continuous wavenumber $k$.

$$\cos(\tilde{k}h) = -A(\alpha)/B(\alpha). \tag{27}$$

Inverting and taking a Taylor series expansion gives (Thompson and Pinsky, 1994)

$$\tilde{k}h = \arccos\left(-A(kh)/B(kh)\right) = kh - \frac{(kh)^3}{24} + O(kh)^5 \tag{28}$$

The numerical wavenumber remains real valued (propagating waves), provided $|A(kh)/B(kh)| < 1$, which requires the continuous wavenumber $k$ to be bounded by the cut-off value, $kh \leq \sqrt{12}$, corresponding to a minimum resolution of just under 2 elements per wavelength, i.e. about $\lambda/h > 2$. Beyond that, $\tilde{k}$ is complex-valued resulting in rapid amplitude decay (evanescent wave). For propagating waves, the numerical wave differs from the exact wave; the relative phase lag (dispersion error) follows from (28), i.e. $(\tilde{k} - k)/k = -\frac{1}{24}(kh)^2 + O(kh)^4$, or $\tilde{k} - k = -\frac{1}{24}(k^3h^2) + O(k^5h^4)$.

*Encyclopedia of Computational Mechanics*. Edited by Erwin Stein, René de Borst and Thomas J.R. Hughes.

*4.2. Mesh Resolution Rules*

In addition to the approximation error with $L^2$-norm of $O(kh)^2$, the error bounds in the Galerkin FEM involve a "pollution" error of $O(k^3h^2)$ that is related to a loss of stability at large wave numbers (Bayliss, Goldstein and Turkel, 1985). For a one-dimensional Helmholtz problem $u'' + k^2u = 0$ on a unit interval, the error of the finite element solution on standard linear elements measured in the $L^2$-norm $||e^h|| = (\int_\Omega |u^h - u|^2\, dx)^{1/2}$ can be estimated as (Ihlenburg and Babuska, 1995):

$$||u^h - u|| \leq C_1(1 + C_2k)h^2||u''|| \tag{29}$$

where $C_1$ and $C_2$ are generic constants. For oscillatory solutions of the Helmholtz equation such that $||u''|| \sim k^2||u||$, it follows that the error in $L^2$-norm is bounded by the approximation error plus a pollution term (Ihlenburg, 1998)

$$||u^h - u|| \leq C_1(kh)^2 + C_2k^3h^2 \tag{30}$$

For large $k$, the error is governed by the second (pollution) term of order $k^3h^2$, similar to the phase error $\tilde{k} - k$ determined by dispersion analysis. The pollution error in the global norms is present even though the non-dimensional wavenumber $kh$ is held fixed with a constant number of elements per wavelength ($\lambda/h$ =constant). In general, however, if the number of elements per wavelength is increased ($kh$ decreased), it follows that global pollution error is also reduced. If one refines the mesh such that $\lambda/h > 2$, the error decreases with constant logarithmic rate. Resolution rules for approximation of a given signal can be formulated locally by bounding the product $kh$ from above; typically, it is suggested that one takes at least ten ($\lambda/h > 10$) elements per wavelength to control local approximation error. In terms of element size $h < \lambda/10$ is recommended. To control the global integral-norm error of finite element solutions, then the pollution term $k^3h^2$ (in non-dimensional form) must also be bounded. A characteristic length scale of the domain, $L$, should be accounted for in the pollution error, so that the bound becomes $(kL)(kh)^2 < P$, where $P$ is an admissible pollution error determined from computational experience (Ihlenburg, 2003).

*4.3. High-order polynomial approximation*

(Thompson and Pinsky (1994); Ihlenburg and Babuska (1997)) show that both dispersion error and the pollution effect can be minimized by using higher-order polynomial approximation (hp-version of FEM and spectral elements). A dispersion analysis similar to that outlined above for linear elements can be carried out for high-order polynomials of order $p$, and after condensation of internal solution unknowns, a dispersion relation of the form (27) is obtained (Thompson and Pinsky, 1994). In general the relative phase error is of the order $O(kh)^{2p}$. The magnitude of the cut-off value $kh$ grows with the increase of approximation order $p$, however, before reaching this value the numerical wavenumber is complex on small intervals called 'stopping bands' (Thompson and Pinsky, 1994); and thus $kh$ should be kept below the first cutoff value of $kh \leq \sqrt{12}$. The approximation error measured in the $H^1$ norm is of the same order as the relative phase error $O(kh/2p)^p$, while the pollution effect is of order $kL\,(kh/2p)^{2p}$, and thus for $p \geq 2$, and small $kh/p$, the pollution effect is small, (Ihlenburg, 1998). Some numerical experiments on the use of $p$-refinement strategies for three-dimensional elasto-acoustic problems are given in (Dey, 2003).

*Encyclopedia of Computational Mechanics*. Edited by Erwin Stein, René de Borst and Thomas J.R. Hughes.

### *4.4. Generalized Galerkin Methods*

For low-order elements, reduced dispersion and pollution error may be achieved using residual-based methods such as Galerkin least squares (GLS) and related methods (Harari and Hughes, 1992c). In the Galerkin-least-squares (GLS) method the variational form is modified by appending residuals of the governing Helmholtz equation to the standard sesquilinear form,

$$B_{GLS}(u,v) = B(u,v) + \tau(\mathcal{L}u, \mathcal{L}v)_{\tilde{\Omega}} \tag{31}$$

with right-hand side,

$$F_{GLS}(v) = F(v) + \tau(f, \mathcal{L}v)_{\tilde{\Omega}} \tag{32}$$

Here, $\mathcal{L} = \nabla^2 + k^2$ is the Helmholtz differential operator, $\tau$ is a mesh parameter yet to be determined, and $(\cdot,\cdot)_{\tilde{\Omega}}$ is the $L^2$ inner product defined with integration over element interiors. The goal is to use discrete dispersion analysis to select $\tau$ to minimize or eliminate phase error in the numerical solution. For a uniform mesh of piecewise linear finite elements in one-dimension, the GLS system matrix has a similar tridiagonal form as the standard Galerkin matrix. For a $\tau$, defined independent of position, a typical stencil is defined as in (26), but with $\alpha$ replaced with $\alpha_{GLS} = kh\sqrt{1-\tau k^2}$. The optimal $\tau$ is then obtained by requiring no phase error, i.e. setting the GLS wavenumber to match the exact wavenumber ($\tilde{k}h = kh$) in (27), resulting in the condition,

$$\cos(kh) = -A(\alpha_{GLS})/B(\alpha_{GLS}) \tag{33}$$

Solving this equation for $\alpha_{GLS}^2$ and equating the result to $(kh)^2(1-\tau k^2)$ gives,

$$\tau = \frac{1}{k^2}\left(1 - \frac{6}{(kh)^2}\frac{1-\cos kh}{2+\cos kh}\right) \tag{34}$$

For uniform meshes this value eliminates phase error completely, thus the error is entirely from interpolation, with no pollution.

For two-dimensional problems, the analysis is performed on a patch of bilinear elements for a uniform square mesh (Thompson and Pinsky, 1995). Inserting bilinear shape functions written in tensor-product form into the GLS variational form leads to the nine-point difference stencil associated with a typical interior patch of four connected elements,

$$(S - (kh)^2(1-\tau k^2)M)u^h(x_i, y_j) = 0 \tag{35}$$

where $S$ and $M$ are two-dimensional linear difference operators emanating from the coefficients of the assembled stiffness and mass matrix. Assuming a plane wave solution with direction $\theta$ and numerical wavenumber $\tilde{k}$,

$$u^h(x_i, y_j) = e^{i\tilde{k}(x\cos\theta + y\sin\theta)} \tag{36}$$

results in the dispersion relation relating $\tilde{k}$ to $k$ and $\theta$.

$$\frac{1}{6}(kh)^2(1-\tau k^2) = \frac{1-\cos\beta_x}{2+\cos\beta_x} + \frac{1-\cos\beta_y}{2+\cos\beta_y} \tag{37}$$

where $(\beta_x, \beta_y) = \tilde{k}h(\cos\theta, \sin\theta)$. The optimal value of $\tau$ is determined by setting $\tilde{k} = k$, i.e., replacing $(\beta_x, \beta_y)$ with $(\alpha_x, \alpha_y) = kh(\cos\theta, \sin\theta)$ in (37), with the result (Thompson and Pinsky, 1995):

$$\tau = \frac{1}{k^2}\left(1 - \frac{6}{(kh)^2}\left(\frac{1-\cos\alpha_x}{2+\cos\alpha_x} + \frac{1-\cos\alpha_y}{2+\cos\alpha_y}\right)\right) \tag{38}$$

*Encyclopedia of Computational Mechanics*. Edited by Erwin Stein, René de Borst and Thomas J.R. Hughes.

For uniform meshes this value eliminates phase error if the exact solution is a plane-wave in the direction $\theta$. Assuming $\theta = 0$, reverts to the 1-D value (34). However, the predominant direction of waves is generally not known a-priori. In this case, the preferred direction of the GLS-FEM is $\theta_0 = \frac{\pi}{8}$. This value reduces phase error at all angles compared to the standard Galerkin-FEM on uniform meshes. For unstructured grids with distorted bilinear elements, the Laplacian operator appearing in (31) is usually neglected and the element size $h_e$ can be taken as an average over the mesh or $h_e = \sqrt{A_e}$, where $A_e$ is the element area. Numerical evidence shows that the GLS-FEM is relatively insensitive to the precise definition of $\tau$: A $\tau$ defined using $\theta_0 = 0$ or $\theta_0 = \frac{\pi}{8}$ in (38) reduces phase error significantly even on adaptive unstructured meshes (Harari *et al.*, 1996). The additional cost of computing the GLS contribution is very small. Proposed values for $\tau$ on triangle, quadratic, and trilinear brick elements are given in (Harari and Nogueira, 2002; Thompson and Pinsky, 1995; Harari *et al.*, 1996).

In (Oberai and Pinsky, 2000) the idea of the GLS-FEM is extended to include the Helmholtz residual in least-squares form over element interiors $\tilde{\Omega}$, plus an additional residual defined over inter-element boundaries $\tilde{\Gamma}$. The variational form assuming negligible Laplacian residual is,

$$B_{\text{res}}(w,u) = B(w,u) + k^4(\tau w, u)_{\tilde{\Omega}} - k^2(\beta w, [\![u_{,n}]\!])_{\tilde{\Gamma}} - k^2(\beta [\![w_{,n}]\!], u)_{\tilde{\Gamma}}$$

where $[\![u_{,n}]\!]$ is the jump in discontinuous gradients across common element edges. Using dispersion analysis on a uniform mesh of bilinear elements, the values which produce a leading order phase error for all plane-wave directions of order $O((kh)^7)$ are given by (Oberai and Pinsky, 2000),

$$\tau = \frac{1}{8k^2}\left(\tau_1 + \tau_2(\xi^2+\eta^2) - 90\xi^2\eta^2\right), \qquad \beta = \frac{1}{8k^2}\left(-20 + 15(\xi^2+\eta^2)\right)$$

where the coefficients $\tau_1(kh)$ and $\tau_2(kh)$ are,

$$\tau_1 = -10 - \frac{13}{6}(kh)^2 - \frac{9}{640}(kh)^4, \qquad \tau_2 = 30 + \frac{9}{4}(kh)^2 - \frac{67}{768}(kh)^4$$

In the above, $\xi, \eta$, denote natural coordinates defined on the bi-unit reference element. Numerical evidence shows that this residual-based method retains its phase accuracy on nonuniform meshes, displaying very little pollution effects. Successful generalization of residual based methods to waves in plate bending elements and acoustic fluid – structure interaction are given in (Thompson and Thangavelu, 2002; Thompson, 2003; Thompson and Sankar, 2001). Many of the generalized Galerkin methods can be derived within the Variational Multiscale framework (Hughes *et al.*, 1998), including the method of residual-free bubbles (Franca *et al.*, 1997), also related to nearly optimal Petrov-Galerkin methods (Barbone and Harari, 2001). Multiscale considerations also underlie the residual-based method in (Oberai and Pinsky, 2000).

### *4.5. Wave-based discretization methods*

Element free methods based on moving least-squares, and partition-of-unity mesh-free methods provide a means to incorporate analytical wave functions within local basis functions. For the Helmholtz equation in two-dimensions solutions can be approximated using increasing numbers of basis functions in the form of plane waves (Melenk and Babuska, 1996; Babuska and Melenk, 1997),

$$\mathcal{W} = \left\{ e^{ik(x\cos\theta_m + y\sin\theta_m)}, \theta_m = \frac{2\pi m}{n}, m = 0, 1, \ldots, n-1, n = 1, 2, \ldots \right\} \tag{39}$$

(Suleau and Bouillard (2000)) have shown that dispersion and pollutions errors can be reduced by adding a sufficient number of plane wave basis functions within the element-free moving least-squares method. Plane-wave basis functions have also been combined with standard finite elements as a partition-of-unity. (Laghrouche, Bettess, Astley (2002)) derive efficient integration schemes for local plane wave basis functions incorporated within a FEM trial space based on a partition-of-unity derived from standard finite element interpolation functions. While reducing dispersion and pollution error, a drawback of these approaches is the potential for ill-conditioning of the resulting system matrices which may disrupt the practical convergence of the method. In the discontinuous enrichment method (Farhat, Harari and Franca, 2001). the standard finite element polynomial field is enriched within each element by adding the plane wave basis functions in (39). Lagrange multipliers are introduced at element interfaces to enforce a weak continuity of the solution. Using element level condensation, the system matrices are reported to be better conditioned than the partition-of-unity methods. The discontinuous enrichment method may also be derived in the framework of multiscale methods (Farhat, Harari and Hetmaniuk, 2003). Other wave-based methods are the weak element method (Goldstein, 1986), the ultra weak variational formulation (Cessenat and Despres, 1998), application of least-squares methods (Stojek, 1998; Monk and Wang, 1999), and the iterative defect-correction meshless method (Lacroix, Bouillard, and Villon, 2003).

## 5. THE EXTERIOR PROBLEM IN UNBOUNDED DOMAINS

For exterior problems defined on unbounded domains, solutions to the Helmholtz equation $(\nabla^2 + k^2)u = 0$, are outgoing at infinity requiring waves to satisfy a radiation condition. This condition is expressed by the *Sommerfeld radiation condition*,

$$\lim_{r\to\infty} r\left(\frac{\partial u}{\partial r} - iku\right) = 0 \tag{40}$$

In the above, $r = \|\boldsymbol{x}\|$ is a radius centered near the sound source. This condition allows only outgoing waves proportional to $\exp(\mathrm{i}kr)$ at infinity. The Sommerfeld condition can also be expressed in the alternative form,

$$\left|\frac{\partial u}{\partial r} - iku\right| = O\left(\frac{1}{R^2}\right) \text{ for } R \to \infty \tag{41}$$

Let $V$ be the domain of an object with boundary $S$. The exterior domain is defined by the unbounded region $\mathcal{R} = \mathbb{R}^3 \setminus V$. In linear scattering problems the acoustic field within $\mathcal{R}$ is decomposed into a known incident field $u^{\text{inc}}$, and a scattered field $u^{\text{s}}$, so that the total field is $u^{\text{tot}} = u^{\text{inc}} + u^{\text{s}}$. The scattered field satisfies both the Helmholtz equation and radiation condition. For a rigid boundary $S$, the normal velocity is zero, so that from (12),

$$\frac{\partial(u^{\text{s}} + u^{\text{inc}})}{\partial n} = 0, \quad \text{or} \quad \frac{\partial u^{\text{s}}}{\partial n} = -\frac{\partial u^{\text{inc}}}{\partial n} \quad \text{on } S \tag{42}$$

In summary, the exterior scattering problem may be stated as, (S): Given $u^{\text{inc}}$; Find $u(\boldsymbol{x}) \in \mathbb{C}$, such that,

$$(\nabla^2 + k^2)\, u = 0, \qquad \text{in } \mathcal{R} = \mathbb{R}^3 \setminus V \tag{43}$$

*Encyclopedia of Computational Mechanics*. Edited by Erwin Stein, René de Borst and Thomas J.R. Hughes.

$$\frac{\partial u}{\partial n} = -\frac{\partial u^{\text{inc}}}{\partial n} \qquad \text{on } S \tag{44}$$

$$\lim_{r\to\infty} r\left(\frac{\partial u}{\partial r} - iku\right) = 0 \tag{45}$$

Here, $u$ represents the scattered field $u^{\text{s}}$.

A natural way of modeling the acoustic region exterior to a scattering/radiating object is to introduce a boundary element discretization of the surface $S$ based on an integral representation of the exact solution in the exterior. Using the free-space Green's function (fundamental solution), $G(x,x') = e^{ik|\boldsymbol{x}-\boldsymbol{x}'|}/|\boldsymbol{x}-\boldsymbol{x}'|$, such that $(\nabla^2 + k^2)G = 4\pi\delta(|\boldsymbol{x}-\boldsymbol{x}'|)$, $\forall \boldsymbol{x}, \boldsymbol{x}' \in \mathcal{R}$, in the boundary kernels, the boundary element method (BEM) only requires surface discretization on $S$, for an arbitrary shaped obstacle; the Sommerfeld condition is automatically satisfied (Ciskowski and Brebbia, 1991; von Estorff, 2000). The direct BEM implementation for the exterior acoustic problem, exhibits fictitious resonance frequencies associated with eigenvalues of the associated interior complement. A strategy to overcome this problem was proposed in (Burton and Miller, 1971), where a combination of Helmholtz and hypersingular integral equations are linearly combined by a parameter scaled by the wave number, (Amini, 1990). The combined integral equation leads to unique solutions for all wave numbers, but may become poorly conditioned at high frequencies (wavenumbers), whereas FEM has no such limitation. Application of the BEM for the acoustic scattering problem requires solution of large, dense, complex linear systems due to the nonlocal support of the fundamental solution. Direct factorization methods are practical only for small systems with few unknowns. For large systems, iterative methods such as GMRES and fast multipole expansion approximations can reduce the computational expense and storage requirements of the BEM.

Complexity estimates (Harari and Hughes, 1992a) and numerical evidence (Burnett, 1994) have shown that domain based methods such as the finite element method (FEM) are an effective alternative to the BEM for exterior acoustics problems; especially for large systems due to the sparse structure of the resulting system matrices. Finite element discretization of the exterior acoustic region also allows for a natural coupling of an acoustic fluid to an elastic radiator/scatterer in applications of structural acoustics.

Domain based methods such as the FEM introduce an artificial boundary $\Gamma$, which divides the original unbounded domain into two regions: a finite computational domain $\Omega$ and an infinite residual region $\mathcal{D} = \mathcal{R}\setminus\Omega$, see Figure 1. Methods for modeling the exterior complement $\mathcal{D} = \mathcal{R} \setminus \Omega$, i.e., the infinite region exterior to the artificial boundary $\Gamma$, can be divided into three main categories: infinite elements, absorbing PML layers, and absorbing (non-reflecting) boundary conditions. Infinite element methods represent the exterior complement by assuming a radial approximation with suitable outgoing wave behavior. Matched absorbing layers attempt to rapidly decay outgoing waves in a relatively thin layer exterior to $\Gamma$. For the non-reflecting (absorbing) boundary conditions, the outgoing wave solution in $\mathcal{D}$ is represented by a relation of the unknown solution and its derivative on the artificial truncation boundary $\Gamma$. Options include matching exact analytical series solutions as used in the nonlocal Dirichlet-to-Neumann (DtN) map, and various local approximations.

Non-reflecting boundary conditions take the general form:

$$\frac{\partial u}{\partial n}(\boldsymbol{x}) = Mu(\boldsymbol{x}), \qquad \boldsymbol{x} \in \Gamma \tag{46}$$

*Encyclopedia of Computational Mechanics*. Edited by Erwin Stein, René de Borst and Thomas J.R. Hughes.

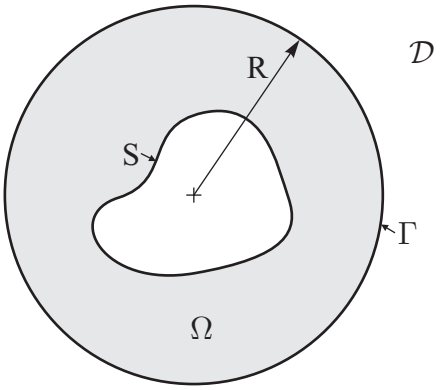


Figure 1. Artificial boundary $\Gamma$ defining finite computational domain $\Omega$ for the exterior problem.

where $M : H^{1/2}(\Gamma) \to H^{-1/2}(\Gamma)$ is a linear operator called the *Dirichlet-to-Neumann* (DtN) map relating Dirichlet data to the outward normal derivative of the solution on $\Gamma$. Physically, the DtN operator $M$ represents the impedance of the exterior region restricted to the boundary $\Gamma$.

Using the DtN map (46), the originally unbounded exterior problem is replaced by an equivalent reduced problem defined on the bounded domain $\Omega$: Given $u^{\text{inc}}$; Find $u(\boldsymbol{x}) \in \mathbb{C}$, such that,

$$(\nabla^2 + k^2)\, u = 0, \qquad \text{in } \Omega \tag{47}$$

$$\frac{\partial u}{\partial n} = -\frac{\partial u^{\text{inc}}}{\partial n}, \qquad \text{on } S \tag{48}$$

$$\frac{\partial u}{\partial n} = Mu, \qquad \text{on } \Gamma \tag{49}$$

The corresponding weak form is, (W): Find $u \in H^1(\Omega)$, such that, for all $w \in H^1(\Omega)$:

$$B(w\,,\,u) - (w, Mu)_{L^2(\Gamma)} = -(w, \frac{\partial u^{\text{inc}}}{\partial n})_{L^2(S)} \tag{50}$$

where

$$B(w\,,\,u) := \int_\Omega (\nabla \bar{w} \cdot \nabla u \;-\; k^2\, \bar{w}\, u)\, \mathrm{d}\boldsymbol{x} \tag{51}$$

and

$$(w, Mu)_{L^2(\Gamma)} = \int_\Gamma \bar{w}\, Mu \; d\Gamma$$

$$(w, \frac{\partial u^{\text{inc}}}{\partial n})_{L^2(S)} = \int_S \bar{w}\, \frac{\partial u^{\text{inc}}}{\partial n}\, \mathrm{d}\boldsymbol{s}$$

A simple approximate condition is to apply the local impedance condition $Mu = iku$, which occurs in the Sommerfeld condition at a finite radius $r = R$. Here,

$$(w, Mu)_{L^2(\Gamma)} = ik \int_\Gamma \bar{u}\, u \; d\Gamma \tag{52}$$

*Encyclopedia of Computational Mechanics*. Edited by Erwin Stein, René de Borst and Thomas J.R. Hughes.

The condition $\mathrm{Im}(ik) > 0$, for all $k > 0$ is sufficient to ensure the well-posedness of the problem. (Harari and Hughes (1992b); Grote and Keller (1995)) show that for the general DtN map, the solution is unique if the inner-product $\mathrm{Im}(u, Mu)_\Gamma > 0$ (or $< 0$), for all $u \in H^{1/2}$, $u \neq 0$. The approximation (52) produces large spurious reflections which pollute the numerical solution unless placed very far from the scattering object. However, a large computational domain is inefficient, leading to a large equation system. Complexity estimates show that it is usually more efficient to use high-order accurate conditions which enable small computational domains. To this end, the artificial boundary $\Gamma$ is often defined in separable coordinates such as a sphere or spheroid, or a rectangular shape in cartesian coordinates. The use of spheroidal or rectangular coordinates allows the artificial boundary to obtain a tight fit around elongated objects. A history on the origins of the DtN finite element method for acoustics and other wave problems in exterior domains is given in (Givoli, 1992; Givoli, 1999).

## 6. THE DtN NON-REFLECTING BOUNDARY CONDITION

The development of the DtN map for a spherical artificial boundary $\Gamma$ is outlined here since it clearly illustrates the main features of the method and can be generalized to other separable coordinates. Consider the exterior region outside an artificial boundary sphere of radius $r = R$,

$$\mathcal{D} = \{R \leq r < \infty\,,\, 0 \leq \theta \leq \pi\,,\, 0 \leq \varphi < 2\pi\} \tag{53}$$

In spherical coordinates, $(x, y, z) = r(\sin\theta\cos\varphi, \sin\theta\sin\varphi, \cos\varphi)$, the wave equation for $u(r, \theta, \varphi, t)$ takes the form,

$$\frac{r^2}{c^2}\frac{\partial^2 u}{\partial t^2} = \frac{\partial}{\partial r}\left(r^2\frac{\partial u}{\partial r}\right) + \Delta_\Gamma u \tag{54}$$

where

$$\Delta_\Gamma u := \frac{1}{\sin\theta}\frac{\partial}{\partial\theta}\left(\sin\theta\frac{\partial u}{\partial\theta}\right) + \frac{1}{\sin^2\theta}\frac{\partial^2 u}{\partial\varphi^2} \tag{55}$$

is the spherical Laplacian operator. Separating variables into radial and angular functions,

$$u(r, \theta, \varphi, t) = f(r, t)\, y(\theta, \varphi) \tag{56}$$

results in two equations with separation constant $\gamma$. The radial function satisfies,

$$\frac{1}{c^2}\frac{\partial^2 f}{\partial t^2} = \frac{\partial^2 f}{\partial r^2} + \frac{2}{r}\frac{\partial f}{\partial r} + \frac{\gamma}{r^2} f, \tag{57}$$

The equation for the angular functions defines an eigenproblem for the spherical Laplacian,

$$\Delta_\Gamma y = \gamma\, y \tag{58}$$

With the conditions $y(\theta, \varphi)$ of period $2\pi$ in $\varphi$, and finite at the poles of the sphere $\theta = 0, \pi$, the eigenvalues are $\gamma = -n(n+1)$, with corresponding eigensolutions for integers $-n \leq m \leq n$, $0 \leq n \leq \infty$, defined up to a constant by $y_{nm} = P_n^m(\cos\theta)e^{im\varphi}$, where $P_n^m(\cos\theta) = P_n^m(\eta)$, are the associated Legendre functions; for $m \geq 0$ the Legendre functions can be generated from Legendre polynomials $P_n(\eta)$, using

$$P_n^m(\eta) = (-1)^m(1-\eta^2)^{m/2}\frac{d^m}{d\eta^m}[P_n(\eta)]. \tag{59}$$

*Encyclopedia of Computational Mechanics*. Edited by Erwin Stein, René de Borst and Thomas J.R. Hughes.

The angular functions form an orthogonal set of eigenfunctions with property,

$$||y_{nm}||^2 = (y_{nm}\,,\, y_{nm})_{\mathcal{S}} := \int_0^{2\pi} \int_0^{\pi} y_{nm}(\theta,\varphi)\, y^*_{nm}(\theta,\varphi)\; d\mathcal{S} = \frac{4\pi}{(2n+1)} \frac{(n+m)!}{(n-m)!}$$

where $d\mathcal{S} = \sin\theta d\theta d\varphi$ denotes the differential surface element on the unit sphere $\mathcal{S}$, parameterized by $0 < \theta < \pi$, $0 < \varphi < 2\pi$. In the above, $y^*_{nm} = P_n^m(\cos\theta)e^{-im\varphi}$ denotes the complex conjugate. An orthonormal set of eigenfunctions is defined by the *spherical harmonics*,

$$Y_{nm}(\theta,\varphi) = \frac{y_{nm}}{||y_{nm}||} = \sqrt{\frac{(2n+1)}{4\pi}\frac{(n-m)!}{(n+m)!}} P_n^m(\cos\theta)e^{im\varphi}$$

The set of spherical harmonics $\{Y_{nm}\}$ is complete and any smooth function $u$ defined over a sphere can be expanded as a convergent series of these eigenfunctions. Thus outside the sphere of radius $R$, the general solution to the wave equation (54) can be expressed by the spherical harmonic expansion,

$$u(r,\theta,\varphi,t) \;=\; \sum_{n=0}^{\infty} \sum_{m=-n}^{n} u_{nm}(r,t)\; Y_{nm}(\theta,\varphi) \tag{60}$$

where $Y_{n,(-m)} = (-1)^m Y^*_{nm}$ and the radial modes, $u_{nm}(r,t) = (u, Y_{nm})_{\mathcal{S}}$ satisfy (57) with $f \to u_{nm}$.

Define a scaled radial coordinate $z = kr$. From the Fourier transform, $\hat{u}(r,\theta,\varphi;\omega) = \mathcal{F}[u(r,\theta,\varphi,t)]$, with the change of dependent variables $w(z) = \sqrt{z}\hat{u}(r)$, $\hat{u}(r) = z^{-1/2}w(z)$, the radial wave equation (57) reduces to *Bessel's differential equation*,

$$\left[\frac{\partial^2}{\partial z^2} + \frac{1}{z}\frac{\partial}{\partial z} + \left(1 - \frac{s^2}{z^2}\right)\right] w = 0 \tag{61}$$

where $s = n + \frac{1}{2}$. Possible solutions are complex-valued Hankel functions of half-integer order defined by, $H_s^{\pm}(z) = J_s(z) \pm iY_s(z)$. Here, $J_s$ and $Y_s$ are standard Bessel and Weber (Neumann) functions of half-integer order, see e.g. (Abramovitz and Stegun, 1964).

The outgoing radiation condition determines the asymptotic behavior as $r \to \infty$. With $s = n + \frac{1}{2}$ and $z = kr$,

$$H_s^+(kr) \sim \sqrt{\frac{2}{\pi kr}} e^{i(kr - s\pi/2 - \pi/4)}, \qquad r \to \infty \tag{62}$$

In conjunction with the time factor $\exp(-i\omega t)$, $H_s^+(kr)$ gives an outgoing wave, while $H_s^-(kr)$ gives an incoming wave. To satisfy the radiation condition, the solution $H_s^-$ is discarded. From here on we shall abbreviate $H_s^+$ simply by $H_s$. Thus the change of variable $\hat{u} = z^{-1/2}w$ leads to the solutions of the form, $\hat{u} = (kr)^{-1/2}H_{n+1/2}(kr)$. By convention *spherical Hankel* functions are defined in terms of these solutions,

$$h_n(kr) := \sqrt{\frac{\pi}{2kr}} H_{n+1/2}(kr) \tag{63}$$

On the spherical boundary $\Gamma$, the solution is then written as a spherical harmonic series,

$$\hat{u}_\Gamma(\theta,\varphi) := \hat{u}(R,\theta,\varphi) = \sum_{n=0}^{\infty} \psi_n(\theta,\varphi) = \sum_{n=0}^{\infty} \sum_{m=-n}^{n} A_{nm}\; Y_{nm}(\theta,\varphi) \tag{64}$$

*Encyclopedia of Computational Mechanics*. Edited by Erwin Stein, René de Borst and Thomas J.R. Hughes.

where,

$$A_{nm} = (\hat{u}, Y_{nm})_{\mathcal{S}} \tag{65}$$

Outside a sphere of radius $R$, the general solution to the Helmholtz equation for the radiated acoustic field is determined by matching the expansion on the spherical boundary $\Gamma$,

$$\hat{u}(r,\theta,\varphi) \;=\; \sum_{n=0}^{\infty} \frac{h_n(kr)}{h_n(kR)} \psi_n(\theta,\varphi). \tag{66}$$

Evaluating the normal derivative on the boundary at $r = R$ gives the DtN map for a spherical truncation boundary (Keller and Givoli, 1989),

$$\frac{\partial \hat{u}}{\partial r} \;=\; \sum_{n=0}^{\infty} \beta_n \psi_n(\theta,\varphi) = \sum_{n=0}^{\infty} \beta_n \sum_{m=-n}^{n} (\hat{u}, Y_{nm})_{\mathcal{S}}\; Y_{nm}(\theta,\varphi) \tag{67}$$

where,

$$\beta_n = k \frac{h_n'(kR)}{h_n(kR)}, \qquad \mathrm{Im}\beta_n > 0 \tag{68}$$

The DtN operator defines an exact non-reflecting condition on the artificial boundary; i.e., there are no spurious reflections introduced at $\Gamma$. The operator is nonlocal since integration is required over the whole surface to compute the coefficients $A_{nm} = (\hat{u}, Y_{nm})_{\mathcal{S}}$.

In practice the DtN map is truncated after a finite number of terms $N$, and is implemented naturally in the variational equation as a symmetric form,

$$\int_{\Gamma} \hat{w} M_N \hat{u}\; d\Gamma = R^2 \sum_{n=0}^{N-1} \beta_n \sum_{m=-n}^{n} (\hat{w}, Y_{nm})_{\mathcal{S}}\; (\hat{u}, Y_{nm})_{\mathcal{S}} \tag{69}$$

The DtN map exactly represents all harmonics in the solution up to the number of terms included in the truncated series expansion as measured by $N$. For higher harmonics $n > N-1$, the truncated DtN models the boundary $\Gamma$ with the homogeneous Neumann condition $\partial\hat{u}/\partial r = 0$ at $r = R$, so that,

$$\int_{\Gamma} \hat{w} M_N(\hat{u})\; d\Gamma = 0, \qquad n > N-1. \tag{70}$$

As a consequence, if an insufficient number of harmonics are included in the series, nonunique solutions may result when $k^2$ matches one of an infinite number of interior resonances (real eigenvalues) associated with the Laplacian operator. (Harari and Hughes (1992b)) showed that this difficulty can be eliminated by setting $N \geq ka$. However, the restriction may require more terms in the DtN map than may be necessary to achieve a desired accuracy, leading to a potential for excessive computation.

This problem is circumvented if a modified truncated DtN operator (Grote and Keller, 1995) is used,

$$M^* = (M_N - B_N) + B \tag{71}$$

where $B$ is any computationally efficient approximation to the DtN operator with the uniqueness property $\mathrm{Im}(u, Bu)_{\Gamma} \neq 0$, and $(M_N - B_N)$ is the truncation of $M - B$ to the first $N$ modes. Suitable operators for $B$ include localizations of the DtN operator and other approximate local absorbing boundary conditions. In the following we develop the modified DtN operator using the first- and second-order local conditions of (Bayliss, Gunzberger and Turkel, 1982).

*Encyclopedia of Computational Mechanics*. Edited by Erwin Stein, René de Borst and Thomas J.R. Hughes.

## 7. THE MODIFIED DtN NON-REFLECTING BOUNDARY CONDITION

The development is based on the idea of annihilating radial terms in a *multipole expansion* for the outgoing solution in powers of $1/kr$. To this end, the spherical Hankel functions can be expressed as (Abramovitz and Stegun, 1964),

$$h_n(z) = (-z)^n \left(\frac{1}{z}\frac{d}{dz}\right)^n h_0(z) = h_0(z) \sum_{j=0}^{n} \frac{g_n^j}{z^j} \tag{72}$$

where

$$h_0(z) = \frac{e^{iz}}{iz}, \qquad g_n^j = (-i)^n (-1)^j \frac{(n+j)!}{(n-j)!} \frac{1}{(2i)^j}$$

In the above, $h_0$ is the spherical Hankel function of zero order and $g_n^j$ are algebraic coefficients.

Substitution of the expression for the Hankel functions (72) into the outgoing series solution (66) and after rearranging results in the multipole expansion, (Atkinson, 1949; Wilcox, 1956):

$$\hat{u}(r,\theta,\varphi;k) \;=\; h_0(kr) \sum_{l=0}^{\infty} \frac{f_l(\theta,\varphi;k)}{(kr)^l} \tag{73}$$

(Bayliss, Gunzberger and Turkel (1982)) showed that a sequence of local differential operators can be used to annihilate terms in this expansion. The first two local BGT operators acting on the expansion for $\hat{u}$, with their corresponding remainders are given by,

$$G_1\hat{u} = \left(\frac{\partial}{\partial r} - B_1\right)\hat{u} = O(1/kr)^3, \qquad G_2\hat{u} = \left(\frac{\partial}{\partial r} + \frac{2}{r} - B_1\right) G_1\hat{u} = O(1/kr)^5 \tag{74}$$

Setting the remainders to zero results in approximate local radiation boundary conditions which may be implemented in standard finite element methods. In the case of the second-order operator, the second-order radial derivative is replaced by the second-order angular derivatives using the Helmholtz equation written in spherical coordinates. Using the operators defined in (74), the corresponding approximate boundary conditions are,

$$\frac{\partial \hat{u}}{\partial r} \;=\; B_1\hat{u}, \qquad B_1 = ik - \frac{1}{r} \tag{75}$$

$$\frac{\partial \hat{u}}{\partial r} \;=\; B_2\hat{u}, \qquad B_2 = (B_1 - \hat{\beta}_1\Delta_\Gamma), \qquad \hat{\beta}_1 = -\frac{1}{2B_1r^2} \tag{76}$$

From the radial orders of the remainders in (74), it is clear that the conditions are more accurate the larger the radius of the artificial boundary. (Thompson and Pinsky (1996)) recognized that these conditions also annihilate up to the first $N = 2$ spherical modes corresponding to $n = 0$ and $n = 1$ in the expansion (66) and thus are equivalent to the first two localized DtN conditions derived in (Harari and Hughes, 1992b), i.e. the DtN coefficients (68), are related by,

$$B_1 = \beta_0 = k\frac{h_0'(kr)}{h_0(kr)} = ik - \frac{1}{r}, \qquad \hat{\beta}_1 = \frac{1}{2}(\beta_1 - \beta_0) = -\frac{1}{2\beta_0 r^2}$$

The first- and second-order BGT conditions have been widely used and have been generalized to spheroidal and arbitrary convex surfaces. Both conditions $B_1$ and $B_2$ satisfy the uniqueness

*Encyclopedia of Computational Mechanics*. Edited by Erwin Stein, René de Borst and Thomas J.R. Hughes.

condition, $\mathrm{Im}(u, Bu)_\Gamma \neq 0$. The local condition $B_2$ is preferred since it is substantially more accurate compared to $B_1$. For spherical boundaries, these conditions tend to be accurate for large $kR$ but inaccurate for small values of $kR$. For spheroidal, (Grote and Keller, 1995) and other convex shapes (Antoine, Barucq and Bendali, 1999), the conditions tend to lose accuracy for higher frequencies (Tezaur *et al.*, 2002). As such, local approximate conditions require careful placement when computing the response over a range of frequencies; the size of the computational domain and the mesh density must be carefully selected to achieve a prescribed accuracy. Direct implementation of local approximate conditions of order higher than two are difficult in conventional finite element methods since they require regularity in angular derivatives higher than $C^0$; see (Givoli, Patlashenko and Keller, 1997).

Both the first-order $B_1$ and second-order $B_2$ local conditions may be used for the operator $B$ in (71), producing a modified DtN condition which provides uniqueness at all wavenumbers irrespective of the number of harmonics $N$ included in the series (69). However the condition $B_2$ is preferred since it provides an improved matrix preconditioner for iterative solvers and gives more accurate solutions when the number of harmonics $N$ used in the truncated DtN series is not sufficient to capture important modes $n > N-1$ in the solution. Applying the local $B_2$ operator to (66) gives the modified DtN:

$$\frac{\partial \hat{u}}{\partial r} = B_2 \hat{u}_\Gamma + \sum_{n=2}^{N-1} \beta_n^{(2)}\, \psi_n(\theta, \varphi) \tag{77}$$

where $\hat{u}_\Gamma$ is the restriction to the boundary at $r = R$, and

$$\beta_n^{(2)} = (\beta_n - \beta_0) - n(n+1)\hat{\beta}_1 \tag{78}$$

are modified DtN coefficients. Note $\beta_0^{(2)} = \beta_1^{(2)} = 0$, so that the summation index may start at $n = 2$, implying that the local $B_2$ BGT operator exactly absorbs the first two harmonics in the outgoing solution. A simpler $B_1$ modified DtN is obtained by setting $\hat{\beta}_1 = 0$, and starting the summation at $n = 1$. The corresponding symmetric form suitable for finite element discretization is,

$$\int_\Gamma \hat{w} M^* \hat{u}\; d\Gamma = B_\Gamma(\hat{w}, \hat{u}) + R^2 \sum_{n=2}^{N-1} \beta_n^{(2)} \sum_{m=-n}^{n} (\hat{w}, Y_{nm})_{\mathcal{S}}\; (\hat{u}, Y_{nm})_{\mathcal{S}} \tag{79}$$

with local term,

$$B_\Gamma(\hat{w}, \hat{u}) := \beta_0 (\hat{w}, \hat{u})_\Gamma + \hat{\beta}_1 R^2 (\nabla^s \hat{w}, \nabla^s \hat{u})_\Gamma \tag{80}$$

The second-order angular derivatives $\Delta_\Gamma$ are reduced to first-order by integration-by-parts on the spherical boundary. In the above,

$$\nabla^s := \frac{1}{h_\theta} \frac{\partial}{\partial \theta} \boldsymbol{e}_\theta + \frac{1}{h_\varphi} \frac{\partial}{\partial \varphi} \boldsymbol{e}_\varphi,$$

and $h_\theta = R$, $h_\varphi = R \sin\theta$. (Grote and Keller (1995)) derived a related modified DtN condition using the second-order BGT operator in native form involving second-order radial derivatives (instead of angular derivatives); a form which is not suitable for standard finite element approximation. For harmonics $n > N-1$, the modified DtN operator is approximated by the local boundary condition,

$$\int_\Gamma \hat{w} M_N^* \hat{u}\; d\Gamma = B_\Gamma(\hat{w}, \hat{u}), \qquad n > N-1 \tag{81}$$

*Encyclopedia of Computational Mechanics*. Edited by Erwin Stein, René de Borst and Thomas J.R. Hughes.

and since Im $B_\Gamma(\hat{u},\hat{u}) \neq 0$, unique solutions are obtained for all harmonics, including $n > N-1$. For high-order modes $n > N-1$ in the solution, the local condition $B_2$ provides an improved approximation compared to $B_1$.

A modified DtN map based on the operator $G_2$ in (74) generalized to spheroidal boundaries is given in (Grote and Keller, 1995) and implemented in a finite difference scheme. The extension of the $B_2$ modified DtN map in spheroidal coordinates suitable for finite element implementation is given in (Thompson, Huan and Ianculescu, 1999); the required radial and angular spheroidal wave functions are readily computed, see e.g. (Zhang and Jianming, 1996).

### *7.1. Finite Element Implementation of Modified DtN*

Using a standard Galerkin approximation $u^h(\boldsymbol{x}) = \boldsymbol{N}^T(\boldsymbol{x})\,\boldsymbol{d}$, where $\boldsymbol{N} \in \mathbb{R}^{N_{dof}}$ is a column vector of standard $C^o$ basis functions, and $\boldsymbol{d} \in \mathbb{C}^{N_{dof}}$ is a column vector containing the $N_{dof}$ unknowns parameters the following indefinite complex-symmetric matrix system results,

$$(\boldsymbol{K}_S + \boldsymbol{K}_{dtn})\boldsymbol{d} = \boldsymbol{f}. \tag{82}$$

where

$$\boldsymbol{K}_S = (\boldsymbol{S} - k^2\boldsymbol{M}) + \boldsymbol{K}_\Gamma$$

is a local sparse matrix, decomposed into a part associated with the discretization of the Helmholtz equation in $\Omega$, defined by the real symmetric arrays $\boldsymbol{S}$ and $\boldsymbol{M}$ defined in (25) and a complex part $\boldsymbol{K}_\Gamma$ associated with the local radiation boundary operator $B_\Gamma$,

$$(\boldsymbol{K}_\Gamma)_{ij} = \beta_0 \int_\Gamma N_i N_j \,\mathrm{d}\Gamma + \hat{\beta}_1 R^2 \int_\Gamma \nabla^s N_i \cdot \nabla^s N_j \,\mathrm{d}\Gamma$$

Additional wavenumber dependent matrices may also be present when using stabilized finite element methods designed for improved accuracy of the discrete wavenumber-frequency relation, e.g., the Galerkin Least-Squares (GLS) and related residual based stabilized methods.

Due to the special structure of the DtN map defined on a separable boundary, the complex-symmetric (non-Hermitian) block matrix $\boldsymbol{K}_{dtn}$ is defined by a summation of vector outer products (rank-1 vector updates),

$$\boldsymbol{K}_{dtn} = \boldsymbol{P}^T\boldsymbol{Z}\boldsymbol{P}, \quad \boldsymbol{Z} = R^2 \sum_{n=2}^{N-1} \beta_n^{(2)} \sum_{m=-n}^{n} \boldsymbol{c}_{nm}\boldsymbol{c}_{nm}^T \tag{83}$$

where $\boldsymbol{c}_{nm} = (\boldsymbol{N}, Y_{nm})_{\mathcal{S}}$ are vectors of size $N_\Gamma$, equal to the number of unknowns on the truncation boundary $\Gamma$, and $\boldsymbol{P}$ is a permutation matrix relating the boundary unknowns to the total number of unknowns.

For a direct solve of (82) , the storage of the full dense matrix $\boldsymbol{K}_{dtn}$, associated with the nonlocal DtN operator, requires $\mathrm{O}(N_\Gamma^2)$ complex numbers. The storage for the sparse matrix $\boldsymbol{K}_S$ is $\mathrm{O}(N_{dof})$, so that the total storage required for $(\boldsymbol{K}_S + \boldsymbol{K}_{dtn})$ is $\mathrm{O}(N_{dof} + N_\Gamma^2)$. For large models, the fully populated submatrix $\boldsymbol{K}_{dtn}$ becomes prohibitively expensive to store and factorize. A similar difficulty is found in the full/dense matrices generated by the boundary element method.

*Encyclopedia of Computational Mechanics*. Edited by Erwin Stein, René de Borst and Thomas J.R. Hughes.

*7.2. Iterative Solution Methods for the Modified DtN*

The situation is significantly different when iterative solution methods are used. Iterative solution methods are generally the algorithm of choice for solving systems with large numbers of unknowns due to significantly reduced storage requirements. Suitable iterative solvers for the indefinite complex symmetric matrix systems arising from discretization of the Helmholtz equation include BiCG-Stab, (Van der Vorst, 1992), and QMR (Freund, 1993) methods. To accelerate convergence of the iterative process, efficient implementations of algebraic and other preconditioners can be constructed based on the sparse matrix $\boldsymbol{K}_S$, (Oberai, Malhotra and Pinsky (1998); Thompson, Huan and Ianculescu (1999)) have shown that the local operator $\boldsymbol{K}_\Gamma$ provides a good approximation to the spectral properties of the complete system matrix, $\boldsymbol{K}_S + \boldsymbol{K}_{dtn}$.

Often the incident field is represented by a plane wave, $u^{\text{inc}}(\boldsymbol{x}) = \exp(ik\boldsymbol{x} \cdot \boldsymbol{\nu})$ propagating along the direction $\boldsymbol{\nu} = (\cos\alpha, \sin\alpha\cos\beta, \sin\alpha\sin\beta)$ with a sweep over different incident directions $\alpha$ and $\beta$. This leads to a problem with fixed left-hand-side matrix and multiple right-hand-side forcing vectors. (Malhotra, Freund and Pinsky (1997)) show how to efficiently solve the multiple right-hand-side problem using a block-QMR algorithm, suitable for the complex symmetric matrix systems arising from discretization of the Helmholtz equation.

The computationally intensive kernel in Krylov subspace iterative solvers is the repeated operation of matrix-by-vector products of the form $\boldsymbol{v}^j = \boldsymbol{Z}\,\boldsymbol{u}^j$, at each iteration $j$. The special structure of the DtN matrix $\boldsymbol{Z}$, as a summation of rank-1 vector updates can be exploited to significantly reduce storage and cost. Here, the vectors $\boldsymbol{c}_{mn}$ can be organized in order and stored as columns in the matrix $\boldsymbol{C}$, of dimension $(N_\Gamma \times N_T)$, where $N_T = N(N+1)$ denote the total number of harmonics included in the truncated DtN expansion. The DtN matrix contribution can then be expressed in the form of a generalized rank-$N_T$ update,

$$\boldsymbol{Z} = \boldsymbol{C}\,\boldsymbol{D}\,\boldsymbol{C}^T \tag{84}$$

where $\boldsymbol{D}$ is a $N_T \times N_T$ diagonal matrix of impedance coefficients, $\beta_n$. Using this construction, a matrix-vector product with the DtN matrix $\boldsymbol{v} = \boldsymbol{Z}\,\boldsymbol{u}$, can be computed efficiently in block form using the following algorithm: 1. Set $\boldsymbol{w} = \boldsymbol{C}^T\boldsymbol{u}$, 2. Set $\boldsymbol{w} = \boldsymbol{D}\boldsymbol{w}$, 3. Set $\boldsymbol{v} = \boldsymbol{C}\boldsymbol{w}$. The dense matrix $\boldsymbol{Z}$ is never assembled; only $\boldsymbol{C}$ and the diagonal coefficients in $\boldsymbol{D}$ need be stored. This implementation avoids the direct evaluation of the full submatrix associated with the unknowns on $\Gamma$ producing significantly reduced storage costs. The storage requirements and number of operations are reduced to $\mathrm{O}(N_{dof} + N_T\,N_\Gamma)$. Since $N_T \ll N_\Gamma$, the storage and cost is considerably lower than a straightforward matrix-vector product. For circular and spherical boundaries, (Oberai, Malhotra and Pinsky, 1998) have shown that a recursive procedure can be used to efficiently generate the discretized angular functions $\boldsymbol{c}_{nm} = (\boldsymbol{N}, Y_{nm})_{\mathcal{S}}$ which allows the use of the DtN condition on $\Gamma$ without any storage penalties related to its nonlocal nature.

(Malhotra and Pinsky (1996)) have shown that the matrix-vector product can also be carried out at the element level, so that standard element-based data structures can be used in the presence of the DtN map. This can be accomplished by localizing element vectors $\boldsymbol{u}^e$, from the global vector $\boldsymbol{u}$, and computing element level matrix-vector products of the form,

$$\boldsymbol{v}^e = \frac{1}{R^2}\sum_{n=2}^{N-1}\beta_n^{(2)}\sum_{m=-n}^{n} a_{mn}\,\boldsymbol{c}_{mn}^e \tag{85}$$

*Encyclopedia of Computational Mechanics*. Edited by Erwin Stein, René de Borst and Thomas J.R. Hughes.

where

$$a_{mn} = \sum_{e=1}^{N_{\Gamma_e}} \boldsymbol{c}^e_{mn} \cdot \boldsymbol{u}^e, \qquad \boldsymbol{c}^e_{mn} = (\boldsymbol{N}^e\,,\, Y_{mn})_{\Gamma_e} \tag{86}$$

Here $N_{\Gamma_e}$ is the number of elements on $\Gamma$, $\Gamma_e = \Omega^e \cap \Gamma$ are element boundaries adjacent to $\Gamma$, and $\boldsymbol{N}^e$ is a column vector of element shape functions. The final global product vector, $\boldsymbol{v}$, is obtained from standard assembly of the local element vectors $\boldsymbol{v}^e$.

## 8. INFINITE ELEMENTS

Another approach to solving the exterior acoustics problem is to replace the non-reflecting boundary condition on $\Gamma$ with a single layer of elements with infinite extent which include an outwardly propagating wavelike factor in their basis functions. Infinite elements have been developed for both separable (e.g. spherical or spheroidal) and nonseparable convex boundaries. The review given below follows (Astley, 2000), here specialized to spherical coordinates. The use of separable coordinates ensures that the trial function is complete as the radial order of the elements increases, and separates the integration of the system matrix coefficient into radial and transverse parts.

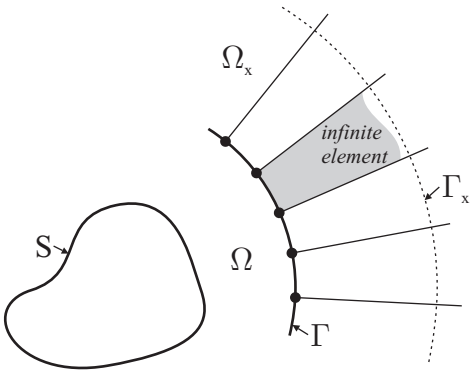


Figure 2. Infinite element topology.

The exterior region is divided into a finite domain $\Omega$ as before where standard finite elements with polynomial basis functions of compact support are used. At an artificial spherical interface $\Gamma$ defined by $r = R$, a single layer of radially oriented infinite elements are extruded from the surface elements on $\Gamma$. The infinite region exterior to $\Gamma$ will be denoted by $\Omega_X$, and is initially taken to be finite with outer radius $X$, which will be extended to infinity $X \to \infty$, see Figure 2.

Assuming a weighting (test) function $w(\boldsymbol{x})$ for $\boldsymbol{x} \in \Omega_X$ which satisfies the Sommerfeld condition (41) at infinity, the weak form may be stated as,

$$K_\Omega(w\,,\,u) + K_{\Omega_X}(w\,,\,u) = F_S(w) \tag{87}$$

Here $K_\Omega$ is the standard sesquilinear form. In $\Omega$, conventional Galerkin finite element discretization with test and trial basis as linear combinations of polynomial functions of

*Encyclopedia of Computational Mechanics*. Edited by Erwin Stein, René de Borst and Thomas J.R. Hughes.

compact support are defined. The form,

$$K_{\Omega_X}(w\,,\,u) := \int_{\Omega_X} (\nabla w \cdot \nabla u \,-\, k^2\, w\, u)\,\mathrm{d}\boldsymbol{x} + ik \int_{\Gamma_X} w\, u\,\mathrm{d}\boldsymbol{s}, \tag{88}$$

is defined for the outer region $\Omega_X$. The approximations for the test and trial solutions in $\Omega_X$ are of the form,

$$w(\boldsymbol{x}) = \sum_{\alpha=1}^{N} c_\alpha w_\alpha(\boldsymbol{x}), \qquad u(\boldsymbol{x}) = \sum_{\beta=1}^{N} d_\beta f_\beta(\boldsymbol{x}),$$

where $w_\alpha(\boldsymbol{x})$ and $f_\alpha(\boldsymbol{x})$ are known basis functions decomposed into products of radial and transverse functions,

$$f_\alpha = F_\nu(r) G_\mu(\theta,\varphi), \qquad w_\alpha = W_\nu(r) G_\mu(\theta,\varphi) \tag{89}$$

for $\nu = 1,\ldots,n$, and $\mu = 1,\ldots,m$; $m$ denotes the number of nodes on the interface $\Gamma$, and $n$ is the number of nodes in the radial direction within the element. Here $G_\mu(\theta,\varphi) = N_\mu(\boldsymbol{x})$ for $\boldsymbol{x}$ restricted to the spherical boundary $\Gamma$, are basis functions which match the finite element surface discretization on $\Gamma$.

Substituting (89) into the weak form gives the system matrix contribution from the infinite elements with coefficients written as tensor products of separable radial and transverse integrals,

$$A_{\alpha\beta} = B^{(1)}_{\nu\nu'} C^{(1)}_{\mu\mu'} + B^{(2)}_{\nu\nu'} C^{(2)}_{\mu\mu'} \tag{90}$$

where

$$C^{(1)}_{\mu\mu'} = (G_\mu\,,\,G_{\mu'})_S, \qquad C^{(2)}_{\mu\mu'} = (\nabla^s G_\mu\,,\,\nabla^s G_{\mu'})_S$$

$$B^{(1)}_{\nu\nu'} = \int_R^X \left( \frac{dW_\nu}{dr}\frac{dF_{\nu'}}{dr} - k^2 W_\nu F_{\nu'} \right) r^2 dr + ikX^2 W_\nu(X) F_{\nu'}(X) \tag{91}$$

$$B^{(2)}_{\nu\nu'} = \int_R^X W_\nu F_{\nu'} dr \tag{92}$$

The radial functions are defined to match the wave character of the Wilcox-Atkinson multipole expansion (73) and thus take the outgoing wave form,

$$F_\nu(r) = R_\nu(\xi) e^{ik(r-R)}$$

Here the radial basis functions $R_\nu(\xi)$ are polynomial functions of order $n$ in the variable $\xi = (R/r)$. The original definition of the radial function was given in terms Lagrange interpolation polynomials in $\xi$ with nodes spaced at prescribed intervals along the radial axis, i.e., $R_\nu(\xi) = \xi L_\nu(\xi)$, where $L_\nu$ are Lagrange interpolation functions at radial nodes. Other options include defining $R_\nu$ as shifted Legendre polynomials in $\xi$, (Shirron and Babuska, 1998), i.e. $R_\nu(\xi) = \xi(1 - P^*_\nu(\xi))$ where $P^*_\nu$ is a shifted Legendre polynomial on the interval $[0,1]$, and explicitly as $R_\nu = \xi^\nu$. The definition does not directly effect the accuracy of the infinite element provided the functions $R_\nu(\xi)$ are independent polynomials of $\xi = (R/r)$. However, the choice preconditions the radial matrices thus greatly affecting the condition number of the resulting coefficient matrix $\boldsymbol{A}$.

*Encyclopedia of Computational Mechanics*. Edited by Erwin Stein, René de Borst and Thomas J.R. Hughes.

The radial test functions have been chosen differently leading to different infinite element formulations.

$$W_\nu(r) = \begin{cases} F_\nu(r), & \text{Bettis} - \text{Burnett Unconjugated} \\ \bar{F}_\nu(r), & \text{Burnett Conjugated} \\ (R/r)^2 \bar{F}_\nu(r), & \text{Astley} - \text{Leis Conjugated (Astley} \textit{et.al.}, 1998) \end{cases}$$

where the bar indicates complex conjugate.

The 'Bettis-Burnett' infinite element defines the test function to be the same as the trial solution basis. (Burnett, 1994) extended the formulation to spheroidal coordinates and was the first researcher to express the shape functions as separable tensor products of radial and transverse functions. In the case of the unconjugated Bettis-Burnett formulation, the radial coefficients $B_{\nu\nu'}$ involve indefinite integrals which require numerical integration.

In the case of the conjugated formulations, the oscillatory plane wave components in the complex conjugate test and trial functions cancel within the integrands so that the the radial coefficients $B_{\nu\nu'}$ may be integrated analytically in closed form resulting in simple expressions leading to system matrices of the form,

$$\boldsymbol{A} = \boldsymbol{K}_X + ik\boldsymbol{C}_X$$

where $\boldsymbol{K}_X, \boldsymbol{C}_X$ are real wavenumber independent sparse matrices (In the case of spheroidal boundaries, an additional matrix $-k^2\boldsymbol{M}_X$ appears). Since the coefficient matrix is proportional to $ik$ and $k^2$, a local time-dependent counterpart is directly available.

The unconjugated formulation of Burnett, regardless on the definition for the radial function $R_\nu$ gives the highest accuracy in the nearfield, yet exhibits ill-conditioning for radial orders greater than about three. In contrast, for the conjugated forms, when using the shifted Legendre polynomials for the radial function stable solutions are possible for higher-orders, (Shirron and Babuska, 1998; Astley, 2000). The Burnett formulation, although highly accurate in the near field for elements of low radial order is inherently unstable (Shirron and Babuska, 1998) as the radial order increases. The conjugated schemes, although less accurate, can be constructed to remain stable and convergent in the far-field (Gerdes, 1998).

## 9. PERFECTLY-MATCHED-LAYER (PML)

The perfectly matched layer (PML) concept originally introduced by (Berenger, 1994) for electromagnetic waves is another option for modeling the far-field for the exterior acoustics problem. The idea is to introduce an exterior layer at an artificial interface such that outgoing plane waves are totally absorbed prior to reaching the outer layer truncation boundary. By splitting the scalar field into nonphysical components and proper selection of damping, the PML equations describe decaying waves, which in theory, assure no reflection occurs at the interface for an arbitrary angle of incidence. The interface and PML are usually formulated in rectilinear Cartesian coordinates, allowing a tight fit around elongated objects. The PML concept has also be generalized to spherical and general curvilinear coordinates. A mathematical analysis of the PML is given in (Abarbanel and Gottlieb, 1997). The development given below follows (Turkel and Yefet, 1998; Harari, Slavutin, and Turkel, 2000), here generalized to three-dimensions.

*Encyclopedia of Computational Mechanics*. Edited by Erwin Stein, René de Borst and Thomas J.R. Hughes.

Starting from the linearized continuity and Euler equations (2) and (4), formally splitting the pressure field $p = p_x + p_y + p_z$, and introducing an artificial absorption term, leads to the PML equations,

$$\frac{1}{c}\dot{\boldsymbol{P}} + [\boldsymbol{\sigma}]\,\boldsymbol{P} = -\rho c \left[\frac{\partial v_x}{\partial x}; \frac{\partial v_y}{\partial y}; \frac{\partial v_z}{\partial z}\right], \qquad \frac{1}{c}\dot{\boldsymbol{v}} + [\boldsymbol{\sigma}]\,\boldsymbol{v} = -\frac{1}{\rho c}\nabla p \tag{93}$$

where $\boldsymbol{P} = [p_x; p_y; p_z]$ is a column array of nonphysical variables, with diagonal absorption matrix, $\boldsymbol{\sigma} = \text{diag}\,\{\sigma_x(x),\, \sigma_y(y),\, \sigma_z(z)\}$. For time-harmonic waves, replace $\frac{\partial}{\partial t} \to -i\omega$ to obtain,

$$\boldsymbol{P} = -\rho c[\boldsymbol{S}]^{-1}\left[\frac{\partial v_x}{\partial x}; \frac{\partial v_y}{\partial y}; \frac{\partial v_z}{\partial z}\right], \qquad \boldsymbol{v} = -\frac{1}{\rho c}[\boldsymbol{S}]^{-1}\nabla p$$

where $\boldsymbol{S} = [\boldsymbol{\sigma} - ik\boldsymbol{I}]$. Eliminating $\boldsymbol{v}$ and using the relation $k^2 p + (-ik)(-ik)(p_x + p_y + p_z) = 0$, leads to a modified Helmholtz equation with complex coordinate transformation,

$$\nabla' \cdot \nabla' p + k^2 p = 0, \qquad \nabla' = \left[\frac{1}{s_x}\frac{\partial}{\partial x}; \frac{1}{s_y}\frac{\partial}{\partial y}; \frac{1}{s_z}\frac{\partial}{\partial z}\right] \tag{94}$$

where $\nabla'$ is a scaled gradient with factor,

$$s_x = (\sigma_x - ik)/(-ik) = 1 + (i\sigma_x)/k$$

Expressions for $s_y$ and $s_z$ are similar with $\sigma_x$ replaced with $\sigma_y$ and $\sigma_z$, respectively. The above reduces to the Helmholtz equation when $\sigma_x = \sigma_y = \sigma_z = 0$. The parameters $\sigma$ are usually taken to vary quadratically from a value of zero at the interface of the physical domain to a maximal value at the truncation of the layer. In layers normal to the $x$-direction, $\sigma_y = \sigma_z = 0$. Only in corner regions are all $\sigma$ values nonzero. Alternatively, the modified Helmholtz equation (94) may be expressed as,

$$\nabla \cdot (\boldsymbol{D}\nabla p) + k^2\, s\, p = 0, \qquad s = s_x\, s_y\, s_z$$

with the diagonal matrix,

$$\boldsymbol{D} = \text{diag}\,\{s_y s_z s_x^{-1},\, s_z s_x s_y^{-1},\, s_x s_y s_z^{-1}\}$$

The corresponding sesquilinear form is,

$$\int_\Omega (\nabla \bar{w} \cdot \boldsymbol{D}\nabla u - k^2\, s\, \bar{w} \cdot u) d\Omega$$

Introduction of finite element discretization leads to standard sparse matrices of complex-symmetric form. There is a compromise between a thin layer which requires a rapid variation of the parameters and a thick layer which requires more grid points. In practice, layers of about 8 points seem to be most common (Turkel and Yefet, 1998). The goal of proper selection of absorption is for the reflection decayed waves off the layer truncation boundary to be less than the truncation error of the numerical approximation. In this case, the solution is relatively insensitive to the boundary conditions applied at the layer truncation. For an arbitrary scattering problem, optimal placement of the interface, layer thickness, and absorption function still appear to be open questions.

*Encyclopedia of Computational Mechanics*. Edited by Erwin Stein, René de Borst and Thomas J.R. Hughes.

## 10. ACCELERATED MULTI-FREQUENCY SOLUTION METHODS

When solving the Helmholtz equation, a wide band of wavenumbers (frequencies) is often required for the system response function. The computational cost of solving the full system response for large systems over several hundred to thousands of distinct wavenumbers can be prohibitively expensive. (Malhotra and Pinsky (2000)) introduced an efficient algorithm for the simultaneous solution of the Helmholtz equation over multiple frequencies in a window using a block Krylov subspace projection method. The approach, which is closely related to matrix Pade approximations, uses a symmetric block Lanczos algorithm to obtain the projection of the problem to a Krylov subspace of much smaller dimension than the original system size. Extension to the unsymmetric case is given in (Wagner *et al.* , 2003, ). The algorithm, which has been applied to both interior and exterior problems modeled with the DtN boundary condition, and has been reported to provide substantial speedup compared to a sequential solution. In (Thompson, Zhang and Ingel, 2001) domain decomposition concepts are combined with interpolation of substructure (subdomain) matrices over frequency bands of interest to accelerate multi-frequency solutions. (Djellouli, Farhat and Tezaur (2001)) give another approach to speedup multi-frequency evaluations by characterizing the derivatives of a scattered field with respect to frequency as the solutions of a reference scattering problem with multiple source terms and local boundary conditions.

## 11. PARALLEL ITERATIVE SOLUTION METHODS

Parallel iterative methods provide a means for dividing the problem into subsystems which when solved in parallel, provide compute time speedup, and for distributed-memory computer systems, the ability to scale-up to very large systems. A computationally intensive kernel in Krylov subspace iterative solvers is the repeated operation of matrix-by-vector products. Partitioning the computational domain into $p$ non-overlapping subdomains (substructures), $\Omega = \bigcup_{i=1}^{p} \Omega_i$, and numbering the nodes interior to the subdomains first, and nodes on the interfaces last, a sparse system matrix-by-vector iterate $\boldsymbol{f} = \boldsymbol{K}_S \boldsymbol{d}$, takes the form of a block arrowhead matrix structure:

$$\begin{Bmatrix} \boldsymbol{f}_1 \\ \boldsymbol{f}_2 \\ \vdots \\ \boldsymbol{f}_p \\ \boldsymbol{f}_v \end{Bmatrix} = \begin{bmatrix} \boldsymbol{A}_1 & & & & \boldsymbol{B}_1 \\ & \boldsymbol{A}_2 & & & \boldsymbol{B}_2 \\ & & \ddots & & \vdots \\ & & & \boldsymbol{A}_p & \boldsymbol{B}_p \\ \boldsymbol{B}_1^T & \boldsymbol{B}_2^T & \cdots & \boldsymbol{B}_p^T & \boldsymbol{A}_v \end{bmatrix} \begin{Bmatrix} \boldsymbol{d}_1 \\ \boldsymbol{d}_2 \\ \vdots \\ \boldsymbol{d}_p \\ \boldsymbol{d}_v \end{Bmatrix} \tag{95}$$

where each $\boldsymbol{d}_i, i = 1, \ldots, p$, represents the subvector of unknowns that are interior to subdomain $\Omega_i$, and $\boldsymbol{d}_v$ represents the vector of all interface unknowns. In the above, $\boldsymbol{A}_i = \boldsymbol{S}_i - k^2 \boldsymbol{M}_i + \boldsymbol{K}_{\Gamma_i}$ are sparse matrices associated with internal unknowns for each subdomain, and $\boldsymbol{A}_v$ is a square matrix associated with unknowns on the interfaces. The global interface matrix $\boldsymbol{A}_v$ is defined as the assembly of contributions of local interface submatrices $A_{v_i}$, but is never explicitly assembled for the iterative solution process. Then $\boldsymbol{B}_i$ are sparse matrices representing the subdomain to interface coupling. In general, the number of interface unknowns $m$ will be considerably less than the number of internal unknowns, $m \ll q$.

*Encyclopedia of Computational Mechanics*. Edited by Erwin Stein, René de Borst and Thomas J.R. Hughes.

For iterative solutions on a parallel computer, the sparse matrix-vector products for each local subdomain can be computed in parallel for each processor $i$,

$$\begin{Bmatrix} \boldsymbol{f}_i \\ \boldsymbol{f}_{v_i} \end{Bmatrix} = \begin{bmatrix} \boldsymbol{A}_i & \boldsymbol{E}_i \\ \boldsymbol{E}_i^T & \boldsymbol{A}_{v_i} \end{bmatrix} \begin{Bmatrix} \boldsymbol{d}_i \\ \boldsymbol{d}_{v_i} \end{Bmatrix} \tag{96}$$

where $A_{v_i}$ and $\boldsymbol{d}_{v_i}$ are local interface subarrays and $\boldsymbol{E}_i$ are local coupling matrices assembled from elements on each subdomain and stored on each distributed processor system. Both the vectors $\boldsymbol{f}_i$ and $\boldsymbol{f}_{v_i}$ can be computed concurrently on each processor. The global interface vector $\boldsymbol{f}_v$ must then be updated by assembly of each subvector $\boldsymbol{f}_{v_i}$. Interprocessor communication is minimized by taking advantage of the fact that nodes on interfaces are shared by only a few local subdomains so that communication for vector updates need only occur between adjacent subdomains sharing common interface data. The above sparse parallel iterative procedures can be used for any of the local absorbing boundary conditions, infinite elements, or PML techniques for treating unbounded domains.

For the DtN matrix $\boldsymbol{K}_{dtn}$, (Ianculescu and Thompson, 2003) showed that the symmetric outer-product structure of the DtN matrix can be exploited when computing the DtN matrix-vector product $\boldsymbol{f}^\Gamma = \boldsymbol{Z}\boldsymbol{d}^\Gamma$, where $\boldsymbol{d}^\Gamma$ is a vector iterate of size $N_\Gamma$. Here the multiplicative split (84) is defined on each subdomain,

$$\boldsymbol{Z}_{ij} = \boldsymbol{C}_i^T \boldsymbol{D} \boldsymbol{C}_j, \quad \boldsymbol{Z}_{v_i v_j} = \boldsymbol{C}_{v_i}^T \boldsymbol{D} \boldsymbol{C}_{v_j} \tag{97}$$

where $\boldsymbol{Z}_{ij}$ and $\boldsymbol{Z}_{v_i v_j}$ are the discretized DtN operators coupling subdomain $i$ with subdomain $j$ and the local interface $v_i$ and $v_j$, respectively, and $\boldsymbol{C}_i$ and $\boldsymbol{C}_{v_i}$ are the restrictions of the matrix angular functions for each subdomain which are computed and stored on each processor concurrently. Extracting the DtN unknowns on the boundary $\boldsymbol{d}^\Gamma$, the DtN matrix-vector product can then be formed as,

$$\begin{Bmatrix} \boldsymbol{f}_i^\Gamma \\ \boldsymbol{f}_{v_i}^\Gamma \end{Bmatrix} = \begin{Bmatrix} \boldsymbol{C}_i \\ \boldsymbol{C}_{v_i} \end{Bmatrix} \boldsymbol{D} \sum_{j=1}^{p} \boldsymbol{u}_j \tag{98}$$

where

$$\boldsymbol{u}_j = \boldsymbol{C}_j^T \boldsymbol{d}_j^\Gamma + \boldsymbol{C}_{v_j}^T \boldsymbol{d}_{v_j}^\Gamma \tag{99}$$

is a vector of size equal to $N_T = N(N+1)$, the total number of harmonics, and computed concurrently on each processor. The summation in (98) is carried out by summing each $\boldsymbol{u}_j$ on each processor $j$ and storing the result back onto each of them (requires all-to-all communication). As a result, collective communication of the nonlocal DtN has been reduced to a relatively small vector of size $N_T \ll N_\Gamma$, independent of the grain size. The computations on the left-side of the summation in (98) are added to the sparse matrix-vector product concurrently on each processor prior to the sparse interface vector update. Using this procedure, the DtN matrix-vector product can be computed with one collective communication per iteration with a vector size equal to the number of harmonics included in DtN series expansion; the effect on the overall communication is roughly that of an extra dot-product communication (The basic BiCG-STAB iteration method for sparse matrices requires two matrix-vector products and six dot-products per iteration).

*Encyclopedia of Computational Mechanics*. Edited by Erwin Stein, René de Borst and Thomas J.R. Hughes.

## 12. DOMAIN DECOMPOSITION METHODS

Domain decomposition methods provide an effective means for problem subdivision for parallel processing. Classical Schur complement based domain-decomposition methods have difficulties when applied to the Helmholtz equation since the inversion of the matrix $\boldsymbol{A}_i = (\boldsymbol{S}_i - k^2\boldsymbol{M}_i)$ defined on each interior subdomain will be singular when the wavenumber corresponds to a resonance frequency (eigenvalue) of the pencil $(\boldsymbol{K}_i, \boldsymbol{M}_i)$. The first resonance will occur at a resolution of less than two subdomains per wavelength (Thompson, Zhang and Ingel, 2001). A domain decomposition method with Sommerfeld-like boundary conditions between subdomains has been proposed by (Susan-Resiga and Atassi, 1998) in an iterative scheme where the nonlocal DtN non-reflecting boundary condition is computed with an iterative lag to maintain sparsity of the parallel subdomain solves.

In (Farhat *et al.*, 2000), a non-overlapping domain decomposition method called FETI-H, based on Lagrange multipliers and alternating subdomain interface conditions is used to solve the Helmholtz equation on parallel computers; the implementation has been restricted to local radiation boundary conditions, e.g. the second-order operator of (Bayliss, Gunzberger and Turkel, 1982). Let $\boldsymbol{d}^{(i)}$ denote the restriction of the unknown vector to subdomain $\Omega_i$, with associated matrices,

$$\boldsymbol{A}^{(i)} = \boldsymbol{S}^{(i)} - k^2\boldsymbol{M}^{(i)} + \boldsymbol{K}_\Gamma^{(i)} + ik\boldsymbol{R}_v^{(i)}$$

This restriction includes both interior and interface unknowns for subdomain $\Omega_i$. Here $\boldsymbol{R}_v^{(i)}$ are regularization matrices defined by radiation transmission conditions at the subdomain interface boundaries,

$$\boldsymbol{d}^{(i)^T}\boldsymbol{R}_v^{(i)}\boldsymbol{d}^{(i)} = \sum_{\substack{j=1\\ j\neq i}}^{p} \epsilon^{ij}\int_{\partial\Omega_i\cap\partial\Omega_j} u^2,\ \epsilon^{ij}\in\{0,\pm 1\},\ \epsilon^{ij} = -\epsilon^{ji}.$$

The use of regularization matrices for the Helmholtz operator is based on the local transmission conditions given in (Benamou and Despres, 1997) and others, and provides for a unique solution on each subdomain.

Introducing the discrete Lagrange multiplier vector $\boldsymbol{\lambda}$ for the constraints equations, $\boldsymbol{C}\hat{\boldsymbol{d}} = 0$, where $\boldsymbol{C} = [\boldsymbol{C}^{(1)}, \ldots, \boldsymbol{C}^{(p)}]$, $\boldsymbol{C}^i$ are signed Boolean matrices with entries 0, $\pm 1$, enforcing continuity of the subdomain solutions across interfaces, leads to the system of linear equations in block matrix form,

$$\begin{bmatrix} \hat{\boldsymbol{A}} & \boldsymbol{C}^T \\ \boldsymbol{C} & 0 \end{bmatrix} \begin{Bmatrix} \hat{\boldsymbol{d}} \\ \boldsymbol{\lambda} \end{Bmatrix} = \begin{Bmatrix} \hat{\boldsymbol{f}} \\ 0 \end{Bmatrix} \tag{100}$$

where $\hat{\boldsymbol{d}}$ is a vector consisting of all subdomain variables, $\hat{\boldsymbol{d}} = (\boldsymbol{d}^{(1)}, \cdots, \boldsymbol{d}^{(p)})$ and $\hat{\boldsymbol{A}} = \mathrm{diag}(\boldsymbol{A}^{(1)}, \ldots, \boldsymbol{A}^{(p)})$ The inclusion of the alternating regularization matrix on the interface boundaries cancel upon global assembly, thus reverting the original problem, and lead to nonsingular and invertible matrices $\boldsymbol{A}^{(i)}$. Eliminating $\hat{\boldsymbol{d}}$ from the first block row and substituting into the second block row leads to the interface problem,

$$\boldsymbol{F}_v\boldsymbol{\lambda} = \boldsymbol{g} \tag{101}$$

*Encyclopedia of Computational Mechanics*. Edited by Erwin Stein, René de Borst and Thomas J.R. Hughes.

where the interface flexibility matrix is defined by,

$$\boldsymbol{F}_v = \boldsymbol{C}\hat{\boldsymbol{A}}^{-1}\boldsymbol{C}^T = \sum_{i=1}^{p} \boldsymbol{C}^{(i)}[\boldsymbol{A}^{(i)}]^{-1}\boldsymbol{C}^{(i)^T} \tag{102}$$

$$\boldsymbol{g} = \boldsymbol{C}\hat{\boldsymbol{A}}^{-1}\hat{\boldsymbol{f}} = \sum_{i=1}^{p} \boldsymbol{C}^{(i)}[\boldsymbol{A}^{(i)}]^{-1}\boldsymbol{f}^{(i)} \tag{103}$$

After (101) is solved for $\lambda$ (using a preconditioned iterative solver), the local solution on each subdomain is computed in parallel from

$$\boldsymbol{d}^{(i)} = [\boldsymbol{A}^{(i)}]^{-1}(\boldsymbol{f}^{(i)} + \boldsymbol{r}^{(i)}) \tag{104}$$

Further details of the parallel implementation and required preconditioning are given in (Farhat *et al.*, 2000; Tezaur, Macedo, and Farhat, 2001).

## 13. DIRECT TIME-DOMAIN METHODS FOR ACOUSTIC WAVES

Spatial discretization of the scalar wave equation leads to the system of second-order differential equations of the form,

$$\boldsymbol{M}\ddot{\boldsymbol{u}}(t) + \boldsymbol{C}\dot{\boldsymbol{u}}(t) + \boldsymbol{K}\boldsymbol{u}(t) = \boldsymbol{f}(t) \tag{105}$$

where the superimposed dot denotes differentiation with respect to time $t$, $\boldsymbol{u}(t)$ is the unknown solution vector, and $\boldsymbol{C}$ is a 'damping' matrix arising from inclusion of an impedance condition. Introducing independent variables $\boldsymbol{y} = (\boldsymbol{u}, \boldsymbol{v})$, $\boldsymbol{v} = \dot{\boldsymbol{u}}$ leads to the first order form,

$$\dot{\boldsymbol{y}}(t) = \boldsymbol{B}\boldsymbol{y}(t) + \boldsymbol{q}(t) \tag{106}$$

where

$$\boldsymbol{B} = -\begin{bmatrix} \boldsymbol{0} & -\boldsymbol{I} \\ \boldsymbol{M}^{-1}\boldsymbol{K} & \boldsymbol{M}^{-1}\boldsymbol{C} \end{bmatrix}, \qquad \boldsymbol{q}(t) = \begin{Bmatrix} \boldsymbol{0} \\ \boldsymbol{M}^{-1}\boldsymbol{f}(t) \end{Bmatrix} \tag{107}$$

The numerical solution to the time-dependent acoustic wave problem may be solved directly using any one of several standard or other time-stepping methods applied to either (105) or (106); both explicit or implicit methods may be used. When using explicit methods $\boldsymbol{M}$ is diagonalized for efficiency. Iterative solvers are effective when using implicit methods due to the local nature of propagating waves, an initial iterate based on a previous time step serves as a good starting value for the next iterate (Astley and Hamilton, 2000; Thompson and He, 2002). Alternatively, spatial and temporal discretization may be applied directly to the general hyperbolic system defined in (5). For acoustic waves propagating over large distances and time, high-order accurate methods are preferred, including hp-FEM and spectral elements in space and high-order accurate time-stepping methods beyond the second-order methods commonly used in structural dynamics applications; effective options are multistage Runge-Kutta methods (Hairer and Wanner, 1991), Taylor-Galerkin methods (Safjan and Oden, 1995) and time-discontinuous Galerkin (TDG) methods (Thompson and He, 2002; Thompson and Pinsky, 1996). Adaptive strategies and associated error estimates used to distribute local space-time elements where needed to accurately track local acoustic waves over large distances and time are reported in (Thompson and He, 2003).

*Encyclopedia of Computational Mechanics*. Edited by Erwin Stein, René de Borst and Thomas J.R. Hughes.

The development of efficient methods for the time-dependent wave equation on unbounded domains has been challenging, particularly because of the need for accurate representation of the time-dependent solution in the domain exterior to the computational domain. To avoid the time-history implied by exact conditions such as the Kirchoff boundary integral method, local (differential) boundary approximations such as the time-dependent counterpart to the operators in (76), have been used (Bayliss and Turkel, 1980). As the order of these local conditions increases they become increasingly difficult to implement due to the occurrence of high-order derivatives. For this reason, they have been limited to simple first and second-order conditions, which for many problems of practical interest give inaccurate solutions.

New boundary treatments have been developed which dramatically improve both the accuracy and efficiency of time domain simulations compared to low-order boundary approximations, e.g. see the review (Hagstrom, 1999). Treatments for nonlinear time-dependent wave problems are reviewed in (Givoli, 1999). Promising approaches include the sequence of exact and asymptotic local boundary operators (Hagstrom and Hariharan, 1998) and their angular harmonic counterparts (Huan and Thompson, 2000; Thompson and Huan, 2000), and those based on Higdon-type conditions (van Joolen, Givoli and Neta, 2003). Each of these methods provide for highly accurate and efficient solution methods for unbounded problems which preserve the sparsity of the matrix equations. Other treatments for the unbounded domain include the use of local infinite elements based on conjugated test functions (Astley *et.al.*, 1998; Astley and Hamilton, 2000), and application of the 'perfectly matched layer' (PML) technique to the system of hyperbolic equations (5), see e.g. (Qi and Geers, 1998). A direct time-domain method for computing far-field solutions is given in (Thompson, Huan and He, 2001).

## 14. CONCLUSIONS

Computational methods for acoustics is an active research area with many recent advances; the reader will note that a majority of references are dated during the last decade. Due to difficulties in accurately resolving wave solutions and controlling pollution effects at high frequencies (wavenumbers), many alternative numerical methods have been proposed, including generalized Galerkin methods, multiscale variational methods, and other wave-based methods based on the partition-of-unity and mesh-free methods. For low-order numerical methods, analytic wavenumber information can be used to derive stabilized methods with improved dispersion (phase) error, and as a consequence, lower pollution error at high wavenumbers. High-order accurate methods including hp-version FEM and spectral element methods may also be used to control numerical dispersion and pollution errors.

For the exterior problem in unbounded domains, methods which model the near field with a domain based numerical method such as the finite element method, together with infinite elements, absorbing PML layers, or nonreflecting boundary conditions deliver accurate and efficient solutions, especially for large scale problems requiring iterative and parallel solution methods and for modeling acoustic-structure interaction. Many of the methods developed for computational acoustics such as the DtN finite element method and infinite elements have been generalized to other wave problems including electromagnetics and elastodynamics. Conversely, some of the most effective methods for modeling acoustics have their origins elsewhere, such as the PML method originally derived for electromagnetic waves.

*Encyclopedia of Computational Mechanics*. Edited by Erwin Stein, René de Borst and Thomas J.R. Hughes.

Several new boundary treatments have been developed which are effective for directly solving the time-dependent acoustic wave equations on unbounded domains. These methods are especially efficient for modeling local wave pulses traveling over large distance and time which would require a large number of solutions in the frequency domain. Direct time-domain methods are also required for nonlinear acoustic waves. In general, high-order methods are preferred over second-order time-stepping methods commonly used in applications of structural dynamics.

## ACKNOWLEDGEMENTS

We would like to thank Isaac Harari for his review and many helpful suggestions which helped improve the presentation and contents of this article.

## REFERENCES

Abarbanel SS and Gottlieb D. A mathematical analysis of the PML method. *J. Comput. Phys.* 1997; **134**(2):357-363.

Abramovitz M and Stegun IA. *Handbook of Mathematical Functions*. National Bureau of Standards, 1964.

Amini S, On the choice of the coupling parameter in boundary integral formulations of the exterior acoustic problem, *Appl. Anal.* 1990; **35**:75-92.

Antoine X, Barucq H and Bendali A. Bayliss-Turkel-like radiation conditions on surfaces of arbitrary shape. *J. Math. Anal. Appl.* 1999; 229(1):184-211.

Astley RJ, Macaulay GJ, Coyette J-P, and Cremers L. Three-dimensional wave-envelope elements of variable order for acoustic radiation and scattering. Part I. Formulation in the frequency domain. *J. Acoust. Soc. Am.*, **103**, (1998), pp. 49-63.

Astley RJ, Macaulay GJ, Coyette J-P, and Cremers L. Three-dimensional wave-envelope elements of variable order for acoustic radiation and scattering. Part II. Formulation in the time domain, *J. Acoust. Soc. Am.*, **103**, (1998), pp. 64-72.

Astley RJ. Infinite elements for wave problems: A review of current formulations and an assessment of accuracy, *Int. J. Numer. Meth. Engng*, **49**, (2000), pp. 951-976

Astley RJ. and Hamilton JA. Numerical studies of conjugated infinite elements for acoustical radiation, *Journal of Computational Acoustics*, 8(1), 1-24 (2000).

Atkinson FV, On Sommerfeld's 'radiation condition'. *the Philosophical Magazine* 40 (1949) 645-651

Babuska I and Melenk JM, The partition of unity method, *Int. J. Numer. Meth. Engng*, 40: 727-758 (1997).

Barbone PE and Harari I. Nearly $H^1$-optimal finite element methods, *Comput. Methods Appl. Mech. Engrg.* 190 (2001) 5679-5690.

Bayliss A and Turkel E. Radiation boundary conditions for wave-like equations, *Commun. Pure Appl. Math.*, **33**, 7707-725, 1980.

Bayliss A, Gunzberger M and Turkel E. Boundary conditions for the numerical solution of elliptic equations in exterior domains, *SIAM J. Appl. Math.* 42 (1982) 430-451.

Bayliss A, Goldstein C and Turkel E. On accuracy conditions for the numerical computation of waves, *J. Comp. Physics* 59 (1985), 396-404.

Benamou JD, Despres B. A domain decomposition method for the Helmholtz equation and related optimal control problems, *J. Comput. Phys.* 136 (1997) 68-82.

Berenger J-P, A perfectly matched layer for the absorption of electromagnetic waves, *J. Comput. Phys.*, 114 (2), 195-200, 1994.

Bouillard P, Ihlenburg F, Error estimation and adaptivity for the finite element method in acoustics: 2D and 3D applications, *Computer Methods in Applied Mechanics and Engineering*, 176, 147-163 (1999).

Burnett D, A 3-D acoustic infinite element based on a generalized multipole expansion, *J. Acoust. Soc. Am.*, **96**, (1994), pp. 2798-2816.

Burton A, and Miller G. The application of integral equation methods to the numerical solution of some exterior boundary-value problems, *Proc. Roy. Soc. London*, Ser A, 323, 1971, pp.201-210.

Cessenat O, and Despres B. Application of an ultra weak variational formulation of elliptic PDEs to the two-dimensional Helmholtz Problem, *SIAM J. Numer. Anal.* 35(1), 255-299, 1998.

Ciskowski RD, Brebbia CA (eds). *Boundary Element Methods in Acoustics*, Computational Mechanics Publications & Elsevier Applied Science: Southampton, 1991.

Dey S. Evaluation of p-FEM approximations for mid-frequency elasto-acoustics, *J. of Computational Acoustics*, 11(2), (2003), pp. 195-225.

Djellouli R, Farhat C and Tezaur R. A fast method for solving acoustic scattering problems in frequency bands, *J. of Computational Physics*, 168, 412-432 (2001).

Farhat C, Macedo A, Lesoinne M, Roux F, Magoules F, La Bourdonnaie A. Two-level domain decomposition methods with Lagrange multipliers for the fast iterative solution of acoustic scattering problems, *Comput. Methods Appl Mech. Engrg.* 184 (2000), 213-239.

Farhat C, Harari I, Franca LP, The discontinuous enrichment method, *Comput. Methods Appl Mech. Engrg.* 190 (2001), 6455-6479.

Farhat C, Harari I, Hetmaniuk U, The discontinuous enrichment method for multiscale analysis, *Comput. Methods Appl Mech. Engrg.* 192 (2003), 3195-3209.

Farhat C, Tezaur R, Djellouli R, On the solution of three-dimensional inverse obstacle acoustic scattering problems by a regularized Newton method, *Inverse Problems* 18 (5): 1229-1246 2002.

Feijoo GR, Malholtra M, Oberai AA, Pinsky PM, Shape sensitivity calculations for exterior acoustics problems, *Engineering Computations*, 18 (3-4): 376-391, 2001.

Filippi P, Habault D, Lefebvre JP, Bergassoli A, *Acoustics: Basic physics, theory and methods*, Academic Press, 1999.

Franca LP, Farhat C, Macedo AP, Lesoinne M. Residual-free bubbles for the Helmholtz equation, *Internat. J. Numer. Methods Engrg.* 40 (21) (1997) 4003-4009.

Freund RW, A transpose-free quasi-minimal residual algorithm for non-hermitian linear systems, *SIAM J. on Sci. Comput.*, 14 (2), (1993) 470-482.

Gerdes K, Conjugated versus the unconjugated infinite element method for the Helmholtz equation in exterior domains, *Comput. Methods Appl. Mech. Engrg.* 152 (1998) 125-145.

Givoli D, *Numerical Methods for Problems in Infinite Domains*, Elsevier: Amsterdam, 1992.

Givoli D, Patlashenko I, and Keller JB, High order boundary conditions and finite elements for infinite domains, *Comput. Methods Appl. Mech. Engrg.*, 143, (1997) 13-39.

Givoli D, Recent Advances in the DtN FE Method, *Archives of Computational Methods in Engineering*, 6 (2), 71-116 (1999).

Goldstein CI, The weak element method applied to Helmholtz type equations, *Appl. Numer. Math.* 2 (1986) 409-426.

Grote MJ and Keller JB, On nonreflecting boundary conditions, *J. of Comput. Phys.*, 122, 231-243, 1995.

*Encyclopedia of Computational Mechanics*. Edited by Erwin Stein, René de Borst and Thomas J.R. Hughes.

Hagstrom T and Hariharan SI, A formulation of asymptotic and exact boundary conditions using local operators, *Appl. Num. Math.* **27**, 403-416, 1998.

Hagstrom T, Radiation boundary conditions for the numerical simulation of waves, *Acta Numerica*, Vol. 8, Cambridge University Press, 1999.

Hairer E and Wanner G, *Solving Ordinary Differential Equations II, Stiff and Differential-Algebraic Problems*, Springer, Berlin, 1991.

Harari I and Hughes TJR. A cost comparison of boundary element and finite element methods for problems of time-harmonic acoustics, *Comp. Meth. Appl. Mech. Eng.* , 97, pp. 77-102, 1992.

Harari I and Hughes TJR. Analysis of Continuous Formulations Underlying the Computation of Time-harmonic Acoustics in Exterior Domains *Comp. Meth. Appl. Mech. Eng.* , 97, pp. 103-124, 1992.

Harari I and Hughes TJR. Galerkin/least-squares finite element methods for the reduced wave equation with non-reflecting boundary conditions in unbounded domains. *Comp. Meth. in Appl. Mech. Eng.* **98**, 411-454 (1992).

Harari I, Grosh K, Hughes TJR, Malhotra M, Pinsky PM, Stewart JR, Thompson LL. Recent Developments in Finite Element Methods for Structural Acoustics, *Archives of Computational Methods in Engineering,* **3**, pp. 132-311, 1996.

Harari I, Slavutin M, Turkel E. Analytical and Numerical Studies of a finite element PML for the Helmholtz Equation. *J. of Computational Acoustics*, 8 (1), 121-137, 2000.

Harari I and Nogueira CL. Reducing dispersion of linear triangular elements for the Helmholtz equation. *J. of Engineering Mechanics*, 128 (3), (2002), 351-358.

Helmholtz H. Theory of air oscillations in tubes with open ends, *R. Reine Angew. Math.*, Vol. 57, 1860; 1-72.

Huan R and Thompson LL. Accurate Radiation Boundary Conditions for the Time-Dependent Wave Equation on Unbounded Domains", *Int. J. Numer. Meth. Engng*, 47, pp. 1569 - 1603, 2000.

Hughes TJR, Feijoo GR, Mazzei L, Quincy J-B, The variational multiscale method – a paradigm for computational mechanics, *Comput. Methods Appl. Mech. Engrg.* 166 (1998) 3-24.

Ianculescu C and Thompson LL. Parallel Iterative Finite Element Solution Methods For Three-Dimensional Acoustic Scattering, *2003 ASME International Mechanical Engineering Congress & Exposition*, Washington, D.C., Nov. 16-21, 2003, Paper IMECE2003-44266.

Ihlenburg F and Babuska I., Dispersion analysis and error estimation of Galerkin finite element methods for the Helmholtz equation, *Int. J. Numer. Meth. Engng* 38, 3745-3774, 1995.

Ihlenburg F and Babuska I, Finite element solution to the Helmholtz equation with high wave numbers - Part II: The hp-pversion of the FEM, *SIAM J. Numer. Anal.* 34 (1), 315-358, 1997.

Ihlenburg F, *Finite Element Analysis of Acoustic Scattering*, Springer-Verlag, 1998.

Ihlenburg F, The medium-frequency range in computational acoustics: practical and numerical aspects, *J. of Computational Acoustics* 11(2), 175-194, 2003.

Junger MC and Feit D, *Sound, structures, and their interaction*, Second Edition, Acoustical Society of America through the American Institute of Physics, 1993.

Keller JB and Givoli D. Exact non-reflecting boundary conditions, *J. Comput. Phys.*, 81, pp. 172-192, 1989.

Laghrouche O, Bettess P, Astley RJ, Modeling of short wave diffraction problems using approximating systems of plane waves, *Int. J. Numer. Meth. Engng*, 54, 1501-1533, 2002.

Lacroix V, Bouillard Ph, and Villon P, An iterative defect-correction type meshless method for acoustics, *Int. J. Numer. Meth. Engng*, 57, 2131-2146, 2003.

Malhotra M and Pinsky PM, A matrix-free interpretation of the nonlocal Dirichlet-to-Neumann radiation boundary condition, *Int. J. Numer. Meth. Engng*, **39**, 3705-3713, 1996.

Malhotra M, Freund RW and Pinsky PM, Iterative solution of multiple radiation and scattering problems in structural acoustics using a block quasi-minimal residual algorithm, *Comp. Methods Appl. Mech. Engrg.* 146 (1997) 173-196.

Malhotra M and Pinsky PM, Efficient computation of multi-frequency far-field solutions of the Helmholtz equation using the Pade approximation, *J. Comput. Acoust.* 8 (2000), 223-240.

Marburg S, Developments in structural-acoustic optimization for passive noise control. *Archives of Computational Methods in Engineering*, 9 (4): 291-370 2001.

Melenk JM and Babuska I, The partition of unity method: basic theory and applications, *Comp. Methods Appl. Mech. Engrg.*, 139, 289-314, 1996.

Monk P, Wang Da-Qing, A least-squares method for the Helmholtz equation, *Comp. Methods Appl. Mech. Engrg.*, 175, 121-136, 1999.

Oberai AA, Malhotra M, Pinsky PM, On the implementation of the Dirichlet-to-Neumann radiation condition for iterative solution of the Helmholtz equation, *Applied Numerical Mathematics*, **27**, 443-464, 1998.

Oberai AA and Pinsky PM, A residual-based finite element method for the Helmholtz equation, *Internat. J. Numer. Methods Engrg.* 2000; 49: 399-419.

Pierce AD, Mathematical Theory of Wave Propagation, *Handbook of Acoustics*, Chapter 2, Edited by Malcolm J. Crocker, John Wiley & Sons, Inc., 1998; 21–45.

Qi Q and Geers TL, Evaluation of the Perfectly Matched Layer for computational acoustics, *J. Comput. Phys.* 139, 166-183 (1998).

Safjan A and Oden JT, High-order Taylor-Galerkin methods for linear hyperbolic systems, *J. Comput. Phys.* 120, 206-230 (1995).

Shirron JJ, Babuska I, A comparison of approximate boundary conditions and infinite element methods for exterior Helmholtz problems, *Comput. Methods Appl. Mech. Engrg.* 1998. 164(1-2): 121-139.

Stojek M, Least-squares trefftz-type elements for the Helmholtz equation, *Int. J. Numer. Methods Engrg.*, 41, (1998) 831-849.

Suleau S and Bouillard P, Dispersion and pollution of meshless solutions for the Helmholtz equation, *Comput. Methods Appl. Mech. Engrg.*, 190, 639-657, (2000).

Susan-Resiga RF, Atassi HM, A domain decomposition method for the exterior Helmholtz problem, *J. Comput. Phys.*, 147, 388-401 (1998).

Stewart JR and Hughes TJR, h-adaptive finite element computation of time-harmonic exterior acoustics problems in two dimensions, *Comput. Methods Appl. Mech. Engrg.*, 146, pp. 65-89, 1997.

Tezaur R, Macedo A, Farhat C, Iterative solution of large-scale acoustic scattering problems with multiple right hand-sides by a domain decomposition method with Lagrange multipliers, *Internat. J. Numer. Methods Engrg.* , 51 (10): 1175-1193, 2001.

Tezaur R, Macedo A, Farhat C, Djellouli R, Three-dimensional finite element calculations in acoustic scattering using arbitrarily shaped convex artificial boundaries. *Internat. J. Numer. Methods Engrg.* , 53 (6) pp. 1461-1476, 2002.

Thompson LL and Pinsky PM, A Space-time finite element method for structural acoustics in infinite domains, Part II: Exact time-dependent non-reflecting boundary conditions, *Comput. Methods in Appl. Mech. Engrg*, Vol 132, pp. 229-258, 1996.

Thompson LL and Sankar S, Dispersion analysis of stabilized finite element methods for acoustic fluid interaction with Reissner-Mindlin plates, *Int. J. Numer. Meth. Engng*, 50, (11), pp. 2521-2545. 2001.

Thompson LL, On Optimal Stabilized MITC4 plate bending elements for accurate frequency response analysis, *Computers & Structures* 81 (2003) 995-1008.

*Encyclopedia of Computational Mechanics*. Edited by Erwin Stein, René de Borst and Thomas J.R. Hughes.

Thompson LL and P.M. Pinsky PM, Complex wavenumber Fourier analysis of the p-version finite element method, *Computational Mechanics*, **13**, No. 4, 255-275 (1994).

Thompson LL and Pinsky PM, A Galerkin least squares finite element method for the two-dimensional Helmholtz equation, *Internat. J. Numer. Methods Engrg.* **38**, (1995) 371-397.

Thompson LL, Huan R, Ianculescu C, Finite element formulation of exact Dirichlet-to-Neumann radiation conditions on elliptic and spheroidal boundaries", *1999 ASME International Mechanical Engineering Congress & Exposition*, Nashville, TN, Nov. 14-19, 1999, ASME Noise Control and Acoustics Division - 1999, NCA-Vol. 26, pp. 497-510.

Thompson LL and Huan R. Computation of far field solutions based on exact nonreflecting boundary conditions for the time-dependent wave equation, *Comput. Methods in Appl. Mech. Engrg* 2000; 190:1551-1577.

Thompson LL, Huan R and He D. Accurate radiation boundary conditions for the two-dimensional wave equation on unbounded domains. *Comput. Methods in Appl. Mech. Engrg* 2001; 191:311-351.

Thompson LL and Thangavelu SR, A stabilized MITC element for accurate wave response in Reissner-Mindlin plates, *Computers & Structures*, 80, (9-10), 769-789, 2002.

Thompson LL and He D, Adaptive time-discontinuous Galerkin methods for acoustic scattering in unbounded domains, *2002 ASME International Mechanical Engineering Congress & Exposition*, New Orleans, Louisiana, Nov. 17-22, 2002, Paper IMECE2002/NCA-32737.

Thompson LL and He D, Local space-time adaptive discontinuous Galerkin finite element methods for time-dependent waves", *2003 ASME International Mechanical Engineering Congress & Exposition*, Washington, D.C., Nov. 16-21, 2003, Paper IMECE2003-42542.

Thompson LL, Zhang L, Ingel RP, Domain decomposition methods with frequency band interpolation for computational acoustics, *2001 ASME International Mechanical Engineering Congress and Exposition*, November 11-16, 2001, New York, New York. The American Society of Mechanical Engineers, IMECE2001, Paper NCA-23532.

Turkel E and Yefet A, Absorbing PML boundary layers for wave-like equations, *Appl. Numer. Math.*, 27 (4), 533-557, 1998.

Van der Vorst HA, Bi-CGSTAB: A fast and smoothly converging variant of Bi-CG for the solution of nonsymmetric linear systems, *SIAM J. Sci. Stat. Comput.*, Vol 13(2), pp. 631-644, 1992.

van Joolen V, Givoli D, Neta B. High-order non-reflecting boundary conditions for dispersive waves in Cartesian, cylindrical and spherical coordinate systems. *International J. of Comput. Fluid Dynamics*, 17 (4): 263-274, 2003.

von Estorff O (ed.) *Boundary Elements in Acoustics: Advances and Applications*, WIT Press: Southampton, 2000.

Wagner MM, Pinsky PM, Malhotra M, Application of Pade via Lanczos approximations for efficient multifrequency solution of Helmholtz problems, *The Journal of the Acoustical Society of America*, Vol 113, 313-319, 2003.

Wilcox CH, An expansion theorem for electromagnetic fields, *Comm. Pure Appl. Math.*, 9, 115-134, 1956.

Williams EG, *Fourier Acoustics, Sound Radiation and Nearfield Acoustical Holography*, Academic Press, 1999.

Zhang S and Jianming J, *Computation of Special Functions*, John Wiley & Sons, Inc. 1996.